Multiple large-scale dynamical pathways for pan–Atlantic compound cold and windy extremes

Jacopo Riboldi[1], Richard Leeding[1], Antonio Segalini[1], and Gabriele Messori[1]

[1]Uppsala University

December 15, 2022

Abstract

Winter cold spells over North America have been correlated with European wind extremes, but the physical mechanisms behind such "pan-Atlantic" compound extremes have not been clarified yet. In this study, we propose that pan–Atlantic cold and windy extremes occur following two possible dynamical pathways. The first one involves the propagation of a Rossby wave train from the Pacific Ocean, associated with windstorms over north-western Europe in the 5-10 days after the cold spell peak. The second is associated with a high-latitude anticyclone over the North Atlantic and an equatorward-shifted jet, leading to windstorms over south-western Europe already in the days preceding the cold spell peak. European windstorms are thus consistently tied to North American cold spells according to the different flow configuration. The analysis underscores that seemingly similar surface extremes may be driven by different processes, and that overlooking these subtleties and conflating them together could lead to misleading conclusions.

Multiple large-scale dynamical pathways for pan–Atlantic compound cold and windy extremes

Jacopo Riboldi[1], Richard Leeding[1], Antonio Segalini[1] and Gabriele Messori[1,2,3]

[1]Department of Earth Sciences, Uppsala University, Uppsala, Sweden
[2]Centre of natural Hazards and Disaster Science (CNDS), Uppsala University, Uppsala, Sweden
[3]Department of Meteorology and Bolin Centre for Climate Research, Stockholm University, Stockholm, Sweden

Key Points:

- North American cold extremes and European windy extremes can be connected physically by two distinct dynamical pathways.
- The first pathway involves Rossby wave propagation from the North Pacific and the cold spell preceding the European windstorm.
- The second pathway features both extremes occurring roughly at the same time thanks to an upper-level anticyclone west of Greenland.

Corresponding author: Jacopo Riboldi, `jacopo.riboldi@geo.uu.se`

Abstract

Winter cold spells over North America have been correlated with European wind extremes, but the physical mechanisms behind such "pan-Atlantic" compound extremes have not been clarified yet. In this study, we propose that pan–Atlantic cold and windy extremes occur following two possible dynamical pathways. The first one involves the propagation of a Rossby wave train from the Pacific Ocean, associated with windstorms over north-western Europe in the 5-10 days after the cold spell peak. The second is associated with a high-latitude anticyclone over the North Atlantic and an equatorward-shifted jet, leading to windstorms over south-western Europe already in the days preceding the cold spell peak. European windstorms are thus consistently tied to North American cold spells according to the different flow configuration. The analysis underscores that seemingly similar surface extremes may be driven by different processes, and that overlooking these subtleties and conflating them together could lead to misleading conclusions.

Plain Language Summary

Previous research noticed cold spells over North America and windstorms over Europe tend to occur within a few days from each other. This connection is supported by the fact that winds usually blow from west to east over the North Atlantic, embedding with them the cyclones modulating the European weather during winter. However, the chain of processes behind this connection remained not fully clarified. Here we explain the complex relationship between the occurrence of North American cold spells and European windstorms. While previous work tried to identify a single physical mechanism, we suggest that two separate pathways can establish a connection between the two types of extremes. The first pathway resembles the initial hypothesis, as the propagation of a train of cyclones and anticyclones from the North Pacific to the North Atlantic sequentially leads to a North American cold spell and, a few days later, to windstorms over north-western Europe. The second pathway, on the other hand, involves an anomalous anticyclone over the North Atlantic, which acts to induce cold spells over North America and windstorms over south-western Europe roughly at the same time: this still leads to a correlation between the two extremes, but without a clear causality direction.

1 Introduction

Cold spells and windstorms are typical examples of cold-season extreme weather events with significant societal and economical impacts (e.g., Karremann et al., 2014; Ryti et al., 2016). The notable winter of 2013/14 featured the co-occurrence of frigid temperatures over North America and of extremely windy and wet conditions over the British Isles, bringing to hypothesize a connection between cold spells over North America and cyclonic activity over western Europe (e.g., Huntingford et al., 2014; Knight et al., 2017). The co-occurrence of cold spells over the United States and of anomalously windy and wet conditions over Europe can be described as a spatially compounding extreme event (Zscheischler et al., 2020), as the two phenomena co-occur over remote regions in a short period of time (Messori et al., 2016; Leeding et al., 2022). The joint occurrence of spatially compounding extremes can magnify their socio-economic impact, exposing actors to correlated losses across their portfolios (e.g., Mills, 2005).

The physical processes behind pan-Atlantic cold and windy extremes likely involves the low-frequency and the transient dynamics of the North Atlantic storm track. Indeed, the continuous generation of cold air over North America during boreal winter modulates the land-sea contrast over the eastern coast of the continent and is a fundamental process for the dynamics of the North Atlantic storm track (Held, 1983; Brayshaw et al., 2009; Portal et al., 2022). However, drivers and possible modulators of this particular type of compound events remain up to now not fully clarified. The work by Messori et al. (2016) selected and composited 60 cold spells over a broad domain in eastern North

America with the aim to study how they could affect the North Atlantic storm track and lead to European wet and windy extremes. Their work highlighted:

1. An intensification, zonalisation, and equatorward shift of the North Atlantic jet stream occuring around the time of the cold spell, resulting in overall enhanced storminess over western Europe.
2. That North American cold spells are associated with a Rossby wave train arching from the North Pacific towards Alaska and then the North Atlantic storm track.
3. Finally, that such an enhancement and equatorward shift of the Atlantic jet stream emerge as statistically significant already five days before the cold spell peak. The presence of a significant European impact (in terms of wind extremes) in the 15 days preceding the cold spell was also noticed by Leeding et al. (2022), who thus hypothesized the presence of a third actor capable of simultaneously driving both sides of the pan-Atlantic extreme.

These results are reminiscent of the pioneering work by Dickson and Namias (1976), who noticed that periods of lower than usual temperature near the eastern coast of the United States were associated with enhanced baroclinicity at the entrance of the North Atlantic storm track. This resulted in extratropical cyclones tracking at lower latitudes than usual, consistently with an *equatorward-shifted* eddy-driven jet stream. On the other hand, the propagation of North Pacific wave trains towards the North Atlantic is known to be associated with a *poleward-shifted* jet stream, projecting approximately onto the positive phase of the North Atlantic Oscillation (NAO; e.g., Franzke et al., 2004; Benedict et al., 2004; Rivière & Orlanski, 2007; Rivière & Drouard, 2015; Schemm et al., 2018). The presence of significant jet stream anomalies over the North Atlantic prior to the peak of the cold spell is also puzzling because, if there indeed was a causal link between cold spells over North America and downstream storm track anomalies, one would expect the storm track response to follow the cold spell in time rather than to anticipate it. Dickson and Namias (1976) can provide a first, plausible hypothesis: they noticed that cold conditions over the eastern coast of North America were tied to the presence of an anticyclone over Greenland, in a configuration resembling the negative phase of the NAO. This potential "upstream" influence of the North Atlantic storm track has been proven to be particularly important for cold spells in the eastern United States, whose likelihood is increased during periods of negative NAO (Cellitti et al., 2006; Smith & Sheridan, 2019; Millin et al., 2022). Based on the literature, we thus hypothesise a complex, two-way interaction between the North Atlantic storm track and North American cold spells, which offers a possible key to interpret the results of (Messori et al., 2016).

This letter aims to elucidate the different drivers of pan-Atlantic cold and windy compound extremes during boreal winter, reconciling the above open questions with our current understanding of the dynamics of the North Atlantic storm track. We show that apparent contradictions likely resulted from the mixing of two different, physically consistent pathways connecting North American cold extremes and European windstorms. For the sake of conciseness, this work will not focus on the joint occurrence of North American cold spells and European precipitation extremes: however, given that wind and precipitation extremes often compound due to extratropical cyclones (Owen et al., 2021), we expect the substance of the results not to change. After an explanation of the employed data and approach (Sec. 2), the circulation pattern associated with the pan-Atlantic extremes is revisited for a representative region over central United States (Sec. 3a). Then, different dynamical pathways associated with the extremes are discussed (Sec. 3b, 3c). The paper is closed by a contextualization of the results and a summary section (Sec. 4).

2 Data and Methods

The analysis is based on ECMWF's ERA5 Reanalysis data (Hersbach et al., 2020), with a spatial resolution of 0.5°×0.5° and a temporal resolution of 1 day between December 1979 and February 2020. Cold spells have been identified following Leeding et al. (2022). They are defined starting from the daily time series of area-averaged 2-meter temperature anomalies during boreal winter (DJF) over 105°-85°W,35°-45°N. This region is chosen because it partly overlaps with the one chosen by Messori et al. (2016), but results are rather insensitive to 5° shifts of the domain in the four cardinal directions (not shown). Anomalies are ranked from the absolute largest to smallest and the time of the strongest anomaly (here defined as t_{CS}) is retained as the cold spell peak. To ensure independence between events, if two or more cold spell peaks occur within 15 days of each other, only the coldest one is retained. The so-defined 35 coldest days in the region are then used for analysis (see Table S1 in the Supporting Information - SI). For a sensitivity analysis to the exact choice of parameters, we refer to Leeding et al. (2022). European surface wind extremes are defined as exceedances of the 98^{th} percentile of 10-meter wind speed for each grid point, with the choice of the percentile threshold following Klawa and Ulbrich (2003). The propagation of low-frequency Rossby wave trains is assessed using the phase-independent formulation of the wave-activity flux (WAF) for stationary, quasi-geostrophic eddies by Takaya and Nakamura (1997). As the resulting wave-activity flux exhibits a significant level of small-scale noise (as noticed also by Wolf & Wirth, 2017), the field was smoothed by retaining only spherical harmonics contributions with $n < 20$ (see Fig. §1 in the SI). More details about the wave-activity flux computation are provided in the SI.

3 Results

3.1 Revisiting the downstream impact of central NA cold spells

Five days before the peak of the central NA cold spells we analyse here, a Rossby wave train propagates from the North Pacific towards North America (anomalous wave-activity flux arrows in Fig. 1a). The wave train features an enhanced Alaskan ridge and an incipient trough to the South of Hudson Bay: these features are consistent with the known dynamics of cold spells over the region (e.g., Carrera et al., 2004; Palmer, 2014; Xie et al., 2017; Millin et al., 2022). A second trough, seemingly unrelated to the North Pacific wave train, is visible west of Europe. This negative streamfunction anomaly is associated with strong upper-level winds at its southern flank, resulting in a significantly enhanced occurrence of extreme surface winds over the Iberian Peninsula and France in the days preceding the cold spell (Fig. 1d).

As the cold spell reaches its peak (t_{CS}) and the Rossby wave train propagates towards the Atlantic, the upper-level jet stream intensifies at the southern edge of the trough over North America and extends eastward (Fig. 1b). Meanwhile, the previously described trough west of Europe merges with the larger one over North America and presumably contributes to the maintenance of an equatorward-shifted jet stream, although significant surface wind extremes are no longer visible over Iberia (Fig. 1e). The propagation of the wave train appears to influence the position and the tilt of the waveguide at the North Atlantic storm track entrance (maximum zonal wind anomaly of $15\,\mathrm{m\,s^{-1}}$, Fig. 1b). The upper-level jet is confined between the trough over North America, directly associated with the cold spell, and the anticyclone located in the subtropics, located at the leading edge of the wave train.

After the cold spell, the trough-ridge system associated with the Rossby wave train continues to shape the North Atlantic waveguide, featuring an enhanced gradient of geostrophic streamfunction and an anomalously strong upper-level jet stream directed towards western Europe (Fig. 1c). This is associated with significant extreme surface wind anoma-

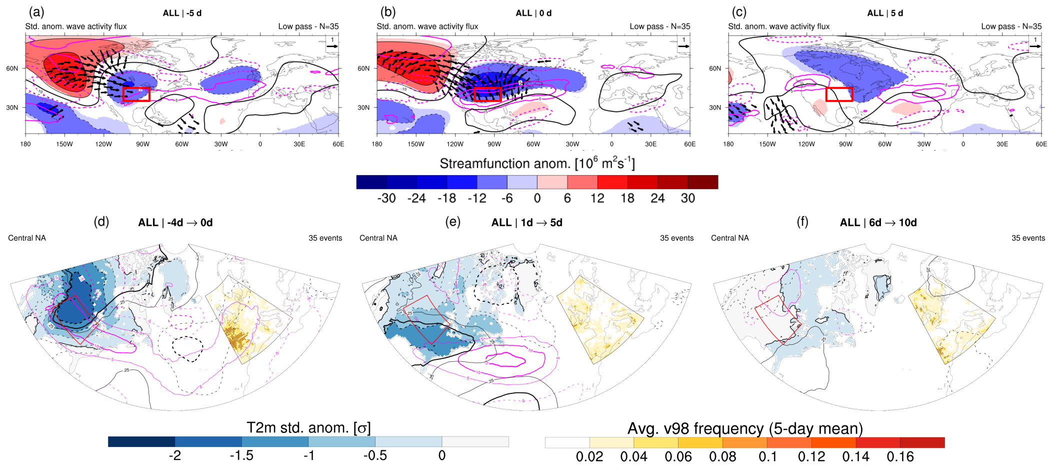

Figure 1. (Top) Lagged composites of 250 hPa wave-activity flux standardized anomalies (arrows), geostrophic streamfunction anomalies (black contours, shaded significant values) and zonal wind anomalies (magenta contours, only $\pm 5\,\mathrm{m\,s^{-1}}$, $\pm 10\,\mathrm{m\,s^{-1}}$, negative values dashed) for the 35 cold spells occurring over the considered central NA region (105°-85°W, 35°-45°N) for (a) t_{CS}-5 d (b) t_{CS}, (c) t_{CS}+5 d. Vectors are shown, and streamfunction anomalies are shaded, only when exceeding the top 99% or bottom 1% of a 2500-times randomly sampled distribution. (Bottom) Composites of extreme (above 98th percentile) 10m wind frequency over Europe, averaged over 5 days, and of standardized 2-meter temperature anomaly over North America and Greenland (notice the two separate color scales) for 5-day periods centered at (d) t_{CS}-2 d, (e) t_{CS}+3 d, (f) t_{CS}+8 d. Overlaid are composites of 250 hPa wind anomaly (magenta contours, only $\pm 5\,\mathrm{m\,s^{-1}}$, $\pm 10\,\mathrm{m\,s^{-1}}$,$\pm 15\,\mathrm{m\,s^{-1}}$), sea level pressure standardized anomaly (black contours, only $\pm 0.25\,\sigma$, $\pm 0.5\,\sigma$), with negative values dashed. Stippling indicates significantly heightened frequency of extreme 5-day-averaged 10m wind with respect to the top 99% or bottom 1% of a 10000-times randomly sampled distribution.

lies over both the British Isles and the Iberian Peninsula (Fig. 1f; see also e.g., Gómara et al., 2014; Messori & Caballero, 2015; Messori et al., 2016). The large-scale configuration projects onto a significantly negative NAO phase in the days preceding the cold spell, but it moves towards more neutral to positive conditions as the cold spell unfolds (Fig. S2a). The anomalous configuration of the upper-level jet stream is also visible using classical jet indices, which indicate a stronger, more equatorward-displaced and zonal jet than usual (as in Figs. Sb-d in the Supplementary Information). The separate trough over western Europe is no longer visible.

In summary, the composites show a wave train upstream of the North American cold spell and the elongation of the North Atlantic jet stream towards western Europe already in the days preceding the cold spell peak, as previously highlighted by Messori et al. (2016). Such a significant anomaly indicates a potential role of North Atlantic storm track dynamics for the genesis of the cold spells; this would however be in apparent contrast, with the role of the North Pacific Rossby wave train as driver of the cold spells, discussed by previous literature.

3.2 Stratification with respect to wave-activity flux

The considerations above suggest a need to compare the relative importance of North Pacific wave trains with respect to the dynamics of the North Atlantic storm track during the cold spells. To verify this, we compute the area-averaged magnitude of the wave-activity flux anomaly vector $|\mathrm{WAF}_{\mathrm{anom}}|$over the considered region (105°-85°W, 35°-45°N) and stratify the same set of cold spells with respect to $|\mathrm{WAF}_{\mathrm{anom}}|$ at cold spell peak. The metric is averaged over the considered cold spell domain, under the assumption that local anomalies in wave-activity flux are indicative of the strength of Rossby wave propagation during the cold spell. We then extract the 12 cold spells associated, respectively, with the top (WAF+) and bottom (WAF-) terciles of $|\mathrm{WAF}_{\mathrm{anom}}|$ and discuss their differences.

A composite analysis shows that cases in the WAF+ subset are indeed characterized by the clear propagation of a Rossby wave train from the North Pacific as the cold spell develops and peaks (Figs. 2a,c). Anomalies in geostrophic streamfunction and wave-activity flux over the north-western portion of North America appear to precede the cold spell also for cases in the WAF- subset, although with a weaker signal than for the WAF+ case (Fig. 2b). The two cold spell subsets are also associated with significantly different flow configurations over the North Atlantic, especially in the days preceding the cold spell (Fig. 2a,b). For WAF+, no significant streamfunction anomalies are visible over the North Atlantic before or during the cold spell peak (Figs. 2a,c). As the wave train propagates over the North Atlantic, the jet tilts poleward over the eastern Atlantic in the direction of the British Isles (Fig. 2e).

The situation is radically different for the WAF- subset. First of all, an anomalous flow pattern resembling a negative NAO phase is visible over the North Atlantic in the days before the cold spell, with an upper-level high over Greenland and two troughs at its southern flanks: one over eastern North America and one over western Europe. Below these, an equatorward-shifted jet is found (Fig. 2b). The unfolding of the WAF- cold spells does not substantially alter the flow configuration over the North Atlantic: the jet remains anomalously equatorward-shifted, and two separate troughs are still visible over the western and eastern parts of the North Atlantic basin (Figs. 2d,f). In this scenario there is no strict need of a precursor North Pacific Rossby wave train: however, the presence of a weak but significant Alaskan ridge in the WAF- composite (Figs. 2b,d) suggests that this feature can still be relevant for particularly intense and/or persistent cold spells.

This analysis explains why central NA cold spells are not followed by a systematically positive or negative NAO (Fig. §3a), as the state of the North Atlantic storm track is conditioned by which dynamical pathway the cold spell is associated with. More pro-

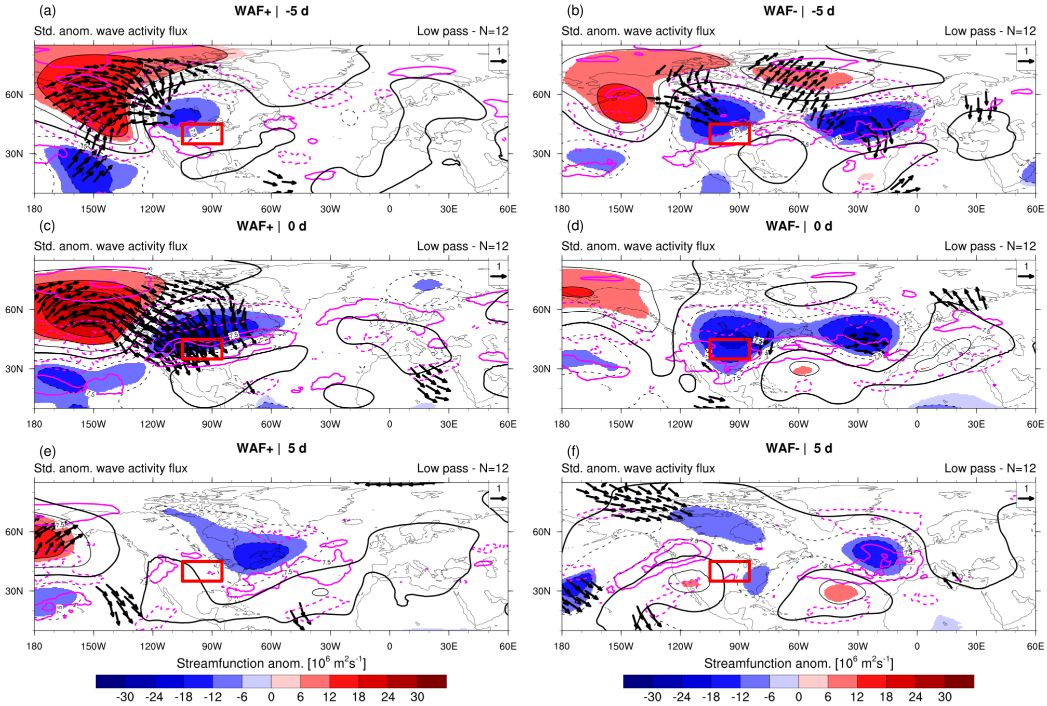

Figure 2. Lagged composites of standardized WAF anomalies (arrows), geostrophic streamfunction anomalies (shaded) and 250 hPa zonal wind anomalies (magenta contours, only $\pm 7.5\,\mathrm{m\,s^{-1}}$, $\pm 15\,\mathrm{m\,s^{-1}}$, negative values dashed) for the 12 central NA cold spells in the (left) WAF+ and (right) WAF- subsets at lags (a,d) t_{CS}-5 d (b,e) t_{CS}, and (c,f) t_{CS}+5 d. Only significant WAF vectors and streamfunction anomalies are shown (with respect to the top 99% or bottom 1% of a 10.000-times randomly sampled distribution).

nounced differences between WAF+ and WAF- emerge when looking at jet speed and latitude, while jet zonality is not systematically different (Figs. §3b-d). As a backward check, we also note that these two distinct dynamical pathways can be re-obtained from a stratification based on the upper and lower terciles of the NAO index four days *after* cold spell peak (see Fig. S4 in the SI). The corresponding 12-cold spell subsets are named NAO+ and NAO-, respectively. The NAO+ cold spells correspond to the NW–SE propagation of a Rossby wave train across North America (Figs. S4a,c), resulting in an enhanced jet stream over the North Atlantic. On the other hand, the NAO- cold spells feature an upper-level anticyclone west of Greenland and an equatorward-shifted jet stream over the Iberian Peninsula already four days before the cold spell peak (Fig. S4b), a situation that remains virtually unchanged as the cold spell unfolds (Figs. S4d,f).

3.3 Implications for surface extremes

The two different dynamical pathways associated with the cold spells are mirrored in differences in the occurrence of European surface wind extremes. In the WAF+ subset, no extreme winds are observed over western Europe preceding the cold spell peak (Figs. 3a,b). This is in sharp contrast with the image gained from the whole subset of the 35 cold spells, which featured a significantly heightened frequency of extreme winds over the Iberian Peninsula and France preceding the cold spell peak (cf. Fig. 1d). On the other hand, the WAF- cold spell subset displays extreme surface winds accompanied by lower than usual sea-level pressure over the Azores and upper-level wind anomalies extending through the whole North Atlantic basin prior to the cold spell peak (Fig. 3d).

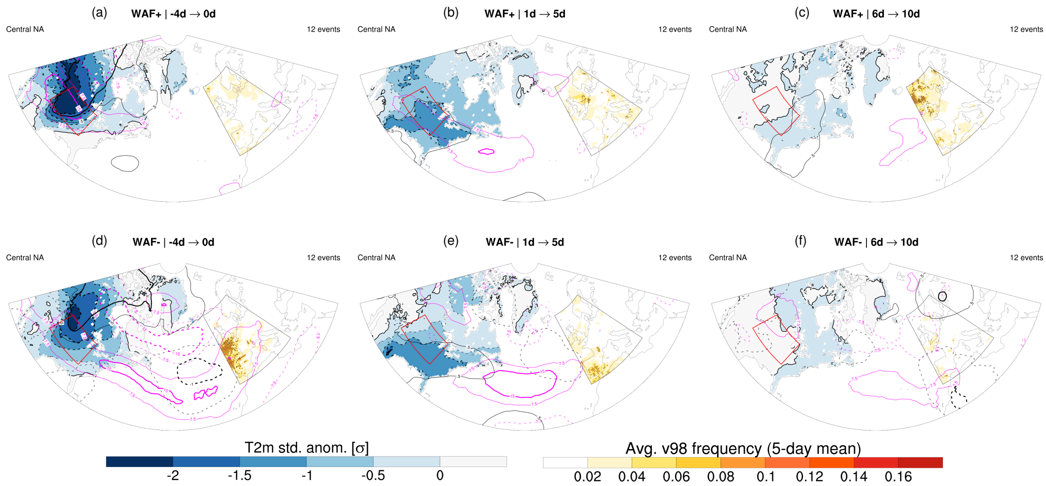

Figure 3. Composites of extreme (above 98th percentile) 10m wind frequency over Europe, averaged over 5 days, and of standardized 2-meter temperature anomaly over North America and Greenland (notice the two separate color scales) following cold spells over central NA belonging to the (top) WAF+ and (bottom) WAF- subsets for the 5-day periods centered at (a,d) t_{CS}-2 d, (b,e) t_{CS}+3 d, (c,f) t_{CS}+8 d. Overlaid are composites of 250 hPa wind anomaly (magenta contours, only $\pm 7.5\,\mathrm{m\,s^{-1}}$, $\pm 15\,\mathrm{m\,s^{-1}}$), sea level pressure standardized anomaly (black contours, only $\pm 0.25\,\sigma$, $\pm 0.5\,\sigma$), with negative values dashed. Stippling indicates 5-day-averaged frequencies of extreme 10m wind exceeding the top 99% or bottom 1% of a randomly sampled distribution.

Indeed, extreme surface winds occur mostly in the period preceding, rather than following, the cold spell peak (Figs. 3e,f). The WAF- subset thus appears characterized by *concurrent* developing cold spells over central NA and extreme surface winds over western Europe. This co-occurrence is likely related to the two troughs visible at the entrance and the exit of the North Atlantic storm track (Figs. 2d,f): while the trough to the west advects cold air at its western flank towards the central NA region, the trough to the east is tied to an upper-level jet streak at its southern flank, associated with extreme winds over the Iberian Peninsula (Figs. 3d,e). In addition, the dynamics portrayed in the WAF- subset are consistent with the streamfunction and jet anomalies visible in the full composite (Fig. 1). We thus hypothesize that the puzzling European wind extremes observed *before* the cold spell peak are mostly related to this second pathway for pan-Atlantic cold and windy extremes, in which the North Atlantic storm track is already in a state conducive to European wind extremes before the cold spell peak is reached over Central NA. Given that the Greenland high is likely emerging from the activity of the North Atlantic storm track, it makes sense that its impacts are felt over Europe first (i.e., in term of windstorms), and then upstream over North America (i.e., in terms of large-scale setup leading to cold spells). This mechanism would explain the anticipated wind impact of central NA cold spells noticed by Messori et al. (2016) and Leeding et al. (2022).

4 Concluding remarks

4.1 Summary

Cold spells over central NA are impactful weather events whose occurrence has been empirically related to windstorms over Europe. The underlying hypothesis was that European windstorms were occurring as a “downstream response” of the “upstream” cold spells. The results of this study challenge this view and allow us to conclude that there

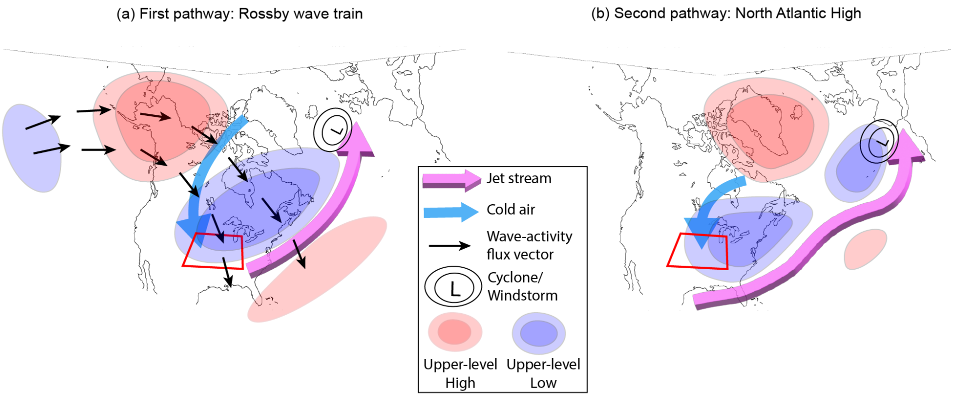

Figure 4. Schematic of the two pathways connecting North American cold spells and European windstorms. (a) In the first pathway, the various upper-level anomalies are related to the propagation of a Rossby wave train from the North Pacific, indicated by the series of thin, black arrows connecting the ridge over Alaska with the trough over eastern North America. (b) In the second pathway, the jet stream is located more equatorward than usual and is associated with anomalous cyclonic activity over south-western Europe.

are at least two possible dynamical pathways to explain the observed statistical link between North American cold spells and European windstorms:

1. Cold spells characterized by the presence of a ridge over Alaska, which is part of a eastward-propagating, low-frequency Rossby wave train, are not associated with significant anomalies over the North Atlantic before cold spell peak. The effect over the North Atlantic storm track manifests itself only when the wave train reaches the eastern portion of the continent, resulting in a tilted, intensified jet stream and in wind extremes over north-western Europe in the 6-10 days following cold spell peak. In this pathway, the propagation of the wave train supports a clear causal link between the circulation pattern causing the cold spell (the Rossby wave train), its impact onto the storm track and the surface wind extremes over Europe (Fig. 4a).
2. The presence of a high west of Greenland is associated with a flow configuration that promotes the development of cold spells over North America and windstorms over Europe at the same time. In particular, the high is often related to the southward displacement of a trough over the eastern United States, which promotes cold air advection at its western flank. At the same time, the large-scale configuration is related to an equatorward shift of the upper-level trough normally associated with the Icelandic Low: this configuration resembles a negative NAO pattern, conducive to extreme winds over south-western Europe (Fig. 4b). As the two weather extremes *co-occur* in time and are associated with a common precursor (the aforementioned Greenland high), it would then be inappropriate to discuss European windstorms as a "downstream effect" of North American cold spells.

In summary, the different drivers of central NA cold spells correspond to different circulation patterns over the North Atlantic, which are then related to an increased frequency of windstorms over different European regions in a physically consistent manner. In the specific case discussed in this study, the original composite picture retained characteristics of the two different drivers at the same time lags, leading to a nonphysical large-scale configuration where the European wind extremes appear to precede the North American cold spell that should cause them. Thus, analyzing pan-Atlantic cold and windy extremes without considering their dynamical drivers can lead to an incomplete, or at worst incorrect, understanding of their dynamics. A similar cautionary argument likely applies to studies concerning temporally and spatially compounding extremes over remote regions (e.g., summer heatwaves or winter cold spells).

4.2 Contextualization of the results and outlook

The two distinct pathways connecting central NA cold spells and European windstorms were identified by stratifying with respect to the area-averaged WAF over the selected cold spell region. Two cold spell subsets were then obtained by selecting the dates corresponding to values in the upper or lower WAF terciles, respectively. Other possible ways to perform this division were attempted, for instance by considering area-averaged wave-activity flux over Alaska, but this choice did not yield a clear division (mainly because not all waves propagating from Alaska engender a cold spell in a given North American region). We thus regard our chosen partition as a simple and physically-grounded way to unravel the different dynamical pathways behind temporally compounding pan-Atlantic cold and windy extremes.

This work focused on a single yet representative North American cold spell domain, but the relative weight of the two pathways likely differs for different regions. Future work will involve a more comprehensive analysis trying to identify differences in the physical connections to European windstorms for cold spells in different North American regions. Another caveat of this analysis is the reduced number of extreme cold spells considered (a total of 35, with 12 cases in the WAF+ and WAF- subsets). We nonetheless underscore the high level of statistical significance of our results. Furthermore, we did not analyse possible remote drivers behind the two identified pathways. Possible candidates are tropical convection anomalies over SE Asia and the maritime continent, which have been linked to the forcing of Rossby wave trains over the Pacific Ocean (e.g., Teng & Branstator, 2017; Riboldi et al., 2022), or the occurrence of sudden stratospheric warmings, which have been connected with the formation of high-latitude anticyclones and with an equatorward displacement of the jet stream over the North Atlantic basin (e.g., Kolstad et al., 2022).

The chosen central NA region is located roughly in the middle between the Pacific and the Atlantic Oceans, and the two identified pathways for pan-Atlantic cold and windy extremes reflect the role played by the basins. The first pathway features a strong wave propagation from the upstream North Pacific, while the second one appears more influenced by high-latitude upper-level ridges over Greenland and the Canadian Arctic, that plausibly result from the dynamics of the North Atlantic storm track (e.g., atmospheric blocking following explosive cyclogenesis). This indicates that both basins can play a role in the genesis of central NA cold spells, as hinted by Lee et al. (2019) and recently emphasized by Millin et al. (2022) using a weather regime approach. This conceptualization has now been extended to the North Atlantic basin, so that pan-Atlantic wet and windy extremes can be seamlessly understood as part of individual large-scale flow configurations tied to the activity of the Pacific and Atlantic storm tracks. In conclusion, this study provided an interesting case-study of the role played by hemispheric-scale teleconnections in coordinating extreme weather events across North America and Europe, paving the way to frameworks for the prediction and mitigation of their joint impacts.

5 Open Research

ERA5 hourly data from 1979-present are available for several pressure levels (Hersbach et al., 2018a) and for surface variables (Hersbach et al., 2018b). Both data sets were freely downloaded from the Copernicus Climate Change Service (C3S) Climate Data Store.

Acknowledgments

JR, RL and GM acknowledge funding from the European Research Council (ERC) under the European Union's Horizon 2020 research and innovation program (grant agreement no. 948309, CENÆ project). The authors also wish to thank Paolo Ghinassi for the helpful discussions about properties of the wave-activity flux.

References

Benedict, J. J., Lee, S., & Feldstein, S. B. (2004). Synoptic view of the North Atlantic Oscillation. *J. Atmos. Sci.*, *61*, 121–144. doi: 10.1175/1520-0469(2004)061⟨0121:SVOTNA⟩2.0.CO;2

Brayshaw, D. J., Hoskins, B., & Blackburn, M. (2009). The basic ingredients of the North Atlantic storm track. Part I: Land–sea contrast and orography. *J. Atmos. Sci.*, *66*, 2539–2558. doi: 10.1175/2009JAS3078.1

Carrera, M. L., Higgins, R. W., & Kousky, V. E. (2004). Downstream weather impacts associated with atmospheric blocking over the northeast pacific. *J. Climate*, *17*, 4823–4839. doi: 10.1175/JCLI-3237.1

Cellitti, M. P., Walsh, J. E., Rauber, R. M., & Portis, D. H. (2006). Extreme cold air outbreaks over the United States, the polar vortex, and the large-scale circulation. *J. Geophys. Res.: Atmospheres*, *111*, D02114. doi: https://doi.org/10.1029/2005JD006273

Dickson, R. R., & Namias, J. (1976). North American influences on the circulation and climate of the North Atlantic sector. *Mon. Wea. Rev.*, *104*, 1255–1265. doi: 10.1175/1520-0493(1976)104⟨1255:NAIOTC⟩2.0.CO;2

Franzke, C., Lee, S., & Feldstein, S. B. (2004). Is the North Atlantic Oscillation a breaking wave? *J. Atmos. Sci.*, *61*, 145–160. doi: 10.1175/1520-0469(2004)061⟨0145:ITNAOA⟩2.0.CO;2

Gómara, I., Rodríguez-Fonseca, B., Zurita-Gotor, P., & Pinto, J. G. (2014). On the relation between explosive cyclones affecting europe and the North Atlantic Oscillation. *Geophys. Res. Lett.*, *41*, 2182–2190. doi: https://doi.org/10.1002/2014GL059647

Held, I. M. (1983). Stationary and quasi-stationary eddies in the extratropical troposphere: Theory. In B. J. Hoskins & R. P. Pearce (Eds.), *Large-Scale Dynamical Processes in the Atmosphere* (pp. 127–168). Academic Press.

Hersbach, H., Bell, B., Berrisford, P., Biavati, G., Horányi, A., Muñoz Sabater, J., . . . Thépaut, J.-N. (2018a). *ERA5 hourly data on pressure levels from 1959 to present.* [dataset]. Copernicus Climate Change Service (C3S) Climate Data Store (CDS). Retrieved from `https://cds.climate.copernicus.eu/cdsapp#!/dataset/reanalysis-era5-pressure-levels?tab=form` doi: 10.24381/cds.bd0915c6

Hersbach, H., Bell, B., Berrisford, P., Biavati, G., Horányi, A., Muñoz Sabater, J., . . . Thépaut, J.-N. (2018b). *ERA5 hourly data on single levels from 1959 to present.* [dataset]. Copernicus Climate Change Service (C3S) Climate Data Store (CDS). Retrieved from `https://cds.climate.copernicus.eu/cdsapp#!/dataset/reanalysis-era5-single-levels?tab=form` doi: 10.24381/cds.adbb2d47

Hersbach, H., Bell, B., Berrisford, P., Hirahara, S., Horányi, A., Muñoz-Sabater, J., . . . Thépaut, J.-N. (2020). The ERA5 global reanalysis. *Quart. J. Roy. Meteor. Soc.*, *146*, 1999–2049. doi: https://doi.org/10.1002/qj.3803

Huntingford, C., Marsh, T., Scaife, A. A., Kendon, E. J., Hannaford, J., Kay, A. L., . . . Allen, M. R. (2014). Potential influences on the United Kingdom's floods of winter 2013/14. *Nature Clim Change*, *4*, 769–777. doi: 10.1038/nclimate231

Karremann, M. K., Pinto, J. G., Reyers, M., & Klawa, M. (2014). Return periods of losses associated with european windstorm series in a changing climate. *En-*

viron. Res. Lett., *9*, 124016. doi: 10.1088/1748-9326/9/12/124016

Klawa, M., & Ulbrich, U. (2003). A model for the estimation of storm losses and the identification of severe winter storms in Germany. *Nat. Hazards Earth Syst. Sci.*, *3*, 725–732. doi: 10.5194/nhess-3-725-2003

Knight, J. R., Maidens, A., Watson, P. A. G., Andrews, M., Belcher, S., Brunet, G., ... Slingo, J. (2017). Global meteorological influences on the record UK rainfall of winter 2013–14. *Env. Res. Lett.*, *12*, 074001. doi: 10.1088/1748-9326/aa693c

Kolstad, E. W., Lee, S. H., Butler, A. H., Domeisen, D. I. V., & Wulff, C. O. (2022). Diverse surface signatures of stratospheric polar vortex anomalies. *J. Geophys. Res.: Atmospheres*, *127*, e2022JD037422. doi: https://doi.org/10.1029/2022JD037422

Lee, S. H., Furtado, J. C., & Charlton-Perez, A. J. (2019). Wintertime North American weather regimes and the Arctic stratospheric polar vortex. *Geophys. Res. Lett.*, *46*, 14892–14900. doi: https://doi.org/10.1029/2019GL085592

Leeding, R., Riboldi, J., & Messori, G. (2022). On pan-Atlantic cold, wet and windy compound extremes. *Wea. Clim. Extremes*. (in press) doi: doi.org/10.1016/j.wace.2022.100524

Messori, G., & Caballero, R. (2015). On double Rossby wave breaking in the North Atlantic. *J. Geophys. Res.: Atmospheres*, *120*, 11,129–11,150. doi: 10.1002/2015JD023854

Messori, G., Caballero, R., & Gaetani, M. (2016). On cold spells in North America and storminess in western Europe. *Geophys. Res. Lett.*, *43*(12), 6620–6628. doi: 10.1002/2016GL069392

Millin, O. T., Furtado, J. C., & Basara, J. B. (2022). Characteristics, evolution, and formation of cold air outbreaks in the great plains of the united states. *J. Climate*, *35*, 4585–4602. doi: 10.1175/JCLI-D-21-0772.1

Mills, E. (2005). Insurance in a climate of change. *Science*, *309*, 1040–1044. doi: 10.1126/science.1112121

Owen, L. E., Catto, J. L., Stephenson, D. B., & Dunstone, N. J. (2021). Compound precipitation and wind extremes over europe and their relationship to extratropical cyclones. *Wea. Clim. Extremes*, *33*, 100342. doi: https://doi.org/10.1016/j.wace.2021.100342

Palmer, T. (2014). Record-breaking winters and global climate change. *Science*, *344*, 803–804. doi: 10.1126/science.1255147

Portal, A., Pasquero, C., D'Andrea, F., Davini, P., Hamouda, M. E., & Rivière, G. (2022). Influence of reduced winter land-sea contrast on the mid-latitude atmospheric circulation. *J. Climate*. (in press) doi: 10.1175/JCLI-D-21-0941.1

Riboldi, J., Rousi, E., D'Andrea, F., Rivière, G., & Lott, F. (2022). Circumglobal rossby wave patterns during boreal winter highlighted by space–time spectral analysis. *Weather Clim. Dynam.*, *3*, 449–469. doi: 10.5194/wcd-3-449-2022

Rivière, G., & Drouard, M. (2015). Dynamics of the Northern Annular Mode at weekly time scales. *J. Atmos. Sci.*, *72*, 4569–4590. doi: 10.1175/JAS-D-15-0069.1

Rivière, G., & Orlanski, I. (2007). Characteristics of the Atlantic storm-track eddy activity and its relation with the North Atlantic Oscillation. *J. Atmos. Sci.*, *64*, 241–266. doi: 10.1175/JAS3850.1

Ryti, N. R., Guo, Y., & Jaakkola, J. J. (2016). Global association of cold spells and adverse health effects: A systematic review and meta-analysis. *Environ. Health Perspect.*, *124*, 12–22. doi: 10.1289/ehp.1408104

Schemm, S., Rivière, G., Ciasto, L. M., & Li, C. (2018). Extratropical cyclogenesis changes in connection with tropospheric ENSO teleconnections to the North Atlantic: Role of stationary and transient waves. *J. Atmos. Sci.*, *75*, 3943–3964. doi: 10.1175/JAS-D-17-0340.1

Smith, E. T., & Sheridan, S. C. (2019). The influence of atmospheric circulation patterns on cold air outbreaks in the eastern United States. *Int. J. Climatol.*, *39*, 2080–2095. doi: https://doi.org/10.1002/joc.5935

Takaya, K., & Nakamura, H. (1997). A formulation of a wave-activity flux for stationary Rossby waves on a zonally varying basic flow. *Geophys. Res. Lett.*, *24*, 2985–2988. doi: https://doi.org/10.1029/97GL03094

Teng, H., & Branstator, G. (2017). Causes of extreme ridges that induce California droughts. *J. Climate*, *30*, 1477–1492. doi: 10.1175/JCLI-D-16-0524.1

Wolf, G., & Wirth, V. (2017). Diagnosing the horizontal propagation of Rossby wave packets along the midlatitude waveguide. *Mon. Wea. Rev.*, *145*, 3247–3264. doi: 10.1175/MWR-D-16-0355.1

Xie, Z., Black, R. X., & Deng, Y. (2017). The structure and large-scale organization of extreme cold waves over the conterminous United States. *Clim. Dyn.*, *49*, 4075–4088. doi: 10.1007/s00382-017-3564-6

Zscheischler, J., Martius, O., Westra, S., Bevacqua, E., Raymond, C., Horton, R. M., … Vignotto, E. (2020). A typology of compound weather and climate events. *Nat. Rev. Earth Environ.*, *1*, 333–347. doi: 10.1038/s43017-020-0060-z

Multiple large-scale dynamical pathways for pan–Atlantic compound cold and windy extremes

Jacopo Riboldi[1], Richard Leeding[1], Antonio Segalini[1] and Gabriele Messori[1,2,3]

[1]Department of Earth Sciences, Uppsala University, Uppsala, Sweden
[2]Centre of natural Hazards and Disaster Science (CNDS), Uppsala University, Uppsala, Sweden
[3]Department of Meteorology and Bolin Centre for Climate Research, Stockholm University, Stockholm, Sweden

Key Points:

- North American cold extremes and European windy extremes can be connected physically by two distinct dynamical pathways.
- The first pathway involves Rossby wave propagation from the North Pacific and the cold spell preceding the European windstorm.
- The second pathway features both extremes occurring roughly at the same time thanks to an upper-level anticyclone west of Greenland.

Corresponding author: Jacopo Riboldi, `jacopo.riboldi@geo.uu.se`

Abstract

Winter cold spells over North America have been correlated with European wind extremes, but the physical mechanisms behind such "pan-Atlantic" compound extremes have not been clarified yet. In this study, we propose that pan–Atlantic cold and windy extremes occur following two possible dynamical pathways. The first one involves the propagation of a Rossby wave train from the Pacific Ocean, associated with windstorms over north-western Europe in the 5-10 days after the cold spell peak. The second is associated with a high-latitude anticyclone over the North Atlantic and an equatorward-shifted jet, leading to windstorms over south-western Europe already in the days preceding the cold spell peak. European windstorms are thus consistently tied to North American cold spells according to the different flow configuration. The analysis underscores that seemingly similar surface extremes may be driven by different processes, and that overlooking these subtleties and conflating them together could lead to misleading conclusions.

Plain Language Summary

Previous research noticed cold spells over North America and windstorms over Europe tend to occur within a few days from each other. This connection is supported by the fact that winds usually blow from west to east over the North Atlantic, embedding with them the cyclones modulating the European weather during winter. However, the chain of processes behind this connection remained not fully clarified. Here we explain the complex relationship between the occurrence of North American cold spells and European windstorms. While previous work tried to identify a single physical mechanism, we suggest that two separate pathways can establish a connection between the two types of extremes. The first pathway resembles the initial hypothesis, as the propagation of a train of cyclones and anticyclones from the North Pacific to the North Atlantic sequentially leads to a North American cold spell and, a few days later, to windstorms over north-western Europe. The second pathway, on the other hand, involves an anomalous anticyclone over the North Atlantic, which acts to induce cold spells over North America and windstorms over south-western Europe roughly at the same time: this still leads to a correlation between the two extremes, but without a clear causality direction.

1 Introduction

Cold spells and windstorms are typical examples of cold-season extreme weather events with significant societal and economical impacts (e.g., Karremann et al., 2014; Ryti et al., 2016). The notable winter of 2013/14 featured the co-occurrence of frigid temperatures over North America and of extremely windy and wet conditions over the British Isles, bringing to hypothesize a connection between cold spells over North America and cyclonic activity over western Europe (e.g., Huntingford et al., 2014; Knight et al., 2017). The co-occurrence of cold spells over the United States and of anomalously windy and wet conditions over Europe can be described as a spatially compounding extreme event (Zscheischler et al., 2020), as the two phenomena co-occur over remote regions in a short period of time (Messori et al., 2016; Leeding et al., 2022). The joint occurrence of spatially compounding extremes can magnify their socio-economic impact, exposing actors to correlated losses across their portfolios (e.g., Mills, 2005).

The physical processes behind pan-Atlantic cold and windy extremes likely involves the low-frequency and the transient dynamics of the North Atlantic storm track. Indeed, the continuous generation of cold air over North America during boreal winter modulates the land-sea contrast over the eastern coast of the continent and is a fundamental process for the dynamics of the North Atlantic storm track (Held, 1983; Brayshaw et al., 2009; Portal et al., 2022). However, drivers and possible modulators of this particular type of compound events remain up to now not fully clarified. The work by Messori et al. (2016) selected and composited 60 cold spells over a broad domain in eastern North

America with the aim to study how they could affect the North Atlantic storm track and lead to European wet and windy extremes. Their work highlighted:

1. An intensification, zonalisation, and equatorward shift of the North Atlantic jet stream occuring around the time of the cold spell, resulting in overall enhanced storminess over western Europe.
2. That North American cold spells are associated with a Rossby wave train arching from the North Pacific towards Alaska and then the North Atlantic storm track.
3. Finally, that such an enhancement and equatorward shift of the Atlantic jet stream emerge as statistically significant already five days before the cold spell peak. The presence of a significant European impact (in terms of wind extremes) in the 15 days preceding the cold spell was also noticed by Leeding et al. (2022), who thus hypothesized the presence of a third actor capable of simultaneously driving both sides of the pan-Atlantic extreme.

These results are reminiscent of the pioneering work by Dickson and Namias (1976), who noticed that periods of lower than usual temperature near the eastern coast of the United States were associated with enhanced baroclinicity at the entrance of the North Atlantic storm track. This resulted in extratropical cyclones tracking at lower latitudes than usual, consistently with an *equatorward-shifted* eddy-driven jet stream. On the other hand, the propagation of North Pacific wave trains towards the North Atlantic is known to be associated with a *poleward-shifted* jet stream, projecting approximately onto the positive phase of the North Atlantic Oscillation (NAO; e.g., Franzke et al., 2004; Benedict et al., 2004; Rivière & Orlanski, 2007; Rivière & Drouard, 2015; Schemm et al., 2018). The presence of significant jet stream anomalies over the North Atlantic prior to the peak of the cold spell is also puzzling because, if there indeed was a causal link between cold spells over North America and downstream storm track anomalies, one would expect the storm track response to follow the cold spell in time rather than to anticipate it. Dickson and Namias (1976) can provide a first, plausible hypothesis: they noticed that cold conditions over the eastern coast of North America were tied to the presence of an anticyclone over Greenland, in a configuration resembling the negative phase of the NAO. This potential "upstream" influence of the North Atlantic storm track has been proven to be particularly important for cold spells in the eastern United States, whose likelihood is increased during periods of negative NAO (Cellitti et al., 2006; Smith & Sheridan, 2019; Millin et al., 2022). Based on the literature, we thus hypothesise a complex, two-way interaction between the North Atlantic storm track and North American cold spells, which offers a possible key to interpret the results of (Messori et al., 2016).

This letter aims to elucidate the different drivers of pan-Atlantic cold and windy compound extremes during boreal winter, reconciling the above open questions with our current understanding of the dynamics of the North Atlantic storm track. We show that apparent contradictions likely resulted from the mixing of two different, physically consistent pathways connecting North American cold extremes and European windstorms. For the sake of conciseness, this work will not focus on the joint occurrence of North American cold spells and European precipitation extremes: however, given that wind and precipitation extremes often compound due to extratropical cyclones (Owen et al., 2021), we expect the substance of the results not to change. After an explanation of the employed data and approach (Sec. 2), the circulation pattern associated with the pan-Atlantic extremes is revisited for a representative region over central United States (Sec. 3a). Then, different dynamical pathways associated with the extremes are discussed (Sec. 3b, 3c). The paper is closed by a contextualization of the results and a summary section (Sec. 4).

2 Data and Methods

The analysis is based on ECMWF's ERA5 Reanalysis data (Hersbach et al., 2020), with a spatial resolution of $0.5° \times 0.5°$ and a temporal resolution of 1 day between December 1979 and February 2020. Cold spells have been identified following Leeding et al. (2022). They are defined starting from the daily time series of area-averaged 2-meter temperature anomalies during boreal winter (DJF) over 105°-85°W,35°-45°N. This region is chosen because it partly overlaps with the one chosen by Messori et al. (2016), but results are rather insensitive to 5° shifts of the domain in the four cardinal directions (not shown). Anomalies are ranked from the absolute largest to smallest and the time of the strongest anomaly (here defined as t_{CS}) is retained as the cold spell peak. To ensure independence between events, if two or more cold spell peaks occur within 15 days of each other, only the coldest one is retained. The so-defined 35 coldest days in the region are then used for analysis (see Table S1 in the Supporting Information - SI). For a sensitivity analysis to the exact choice of parameters, we refer to Leeding et al. (2022). European surface wind extremes are defined as exceedances of the 98^{th} percentile of 10-meter wind speed for each grid point, with the choice of the percentile threshold following Klawa and Ulbrich (2003). The propagation of low-frequency Rossby wave trains is assessed using the phase-independent formulation of the wave-activity flux (WAF) for stationary, quasi-geostrophic eddies by Takaya and Nakamura (1997). As the resulting wave-activity flux exhibits a significant level of small-scale noise (as noticed also by Wolf & Wirth, 2017), the field was smoothed by retaining only spherical harmonics contributions with $n < 20$ (see Fig. §1 in the SI). More details about the wave-activity flux computation are provided in the SI.

3 Results

3.1 Revisiting the downstream impact of central NA cold spells

Five days before the peak of the central NA cold spells we analyse here, a Rossby wave train propagates from the North Pacific towards North America (anomalous wave-activity flux arrows in Fig. 1a). The wave train features an enhanced Alaskan ridge and an incipient trough to the South of Hudson Bay: these features are consistent with the known dynamics of cold spells over the region (e.g., Carrera et al., 2004; Palmer, 2014; Xie et al., 2017; Millin et al., 2022). A second trough, seemingly unrelated to the North Pacific wave train, is visible west of Europe. This negative streamfunction anomaly is associated with strong upper-level winds at its southern flank, resulting in a significantly enhanced occurrence of extreme surface winds over the Iberian Peninsula and France in the days preceding the cold spell (Fig. 1d).

As the cold spell reaches its peak (t_{CS}) and the Rossby wave train propagates towards the Atlantic, the upper-level jet stream intensifies at the southern edge of the trough over North America and extends eastward (Fig. 1b). Meanwhile, the previously described trough west of Europe merges with the larger one over North America and presumably contributes to the maintenance of an equatorward-shifted jet stream, although significant surface wind extremes are no longer visible over Iberia (Fig. 1e). The propagation of the wave train appears to influence the position and the tilt of the waveguide at the North Atlantic storm track entrance (maximum zonal wind anomaly of $15\,\mathrm{m\,s^{-1}}$, Fig. 1b). The upper-level jet is confined between the trough over North America, directly associated with the cold spell, and the anticyclone located in the subtropics, located at the leading edge of the wave train.

After the cold spell, the trough-ridge system associated with the Rossby wave train continues to shape the North Atlantic waveguide, featuring an enhanced gradient of geostrophic streamfunction and an anomalously strong upper-level jet stream directed towards western Europe (Fig. 1c). This is associated with significant extreme surface wind anoma-

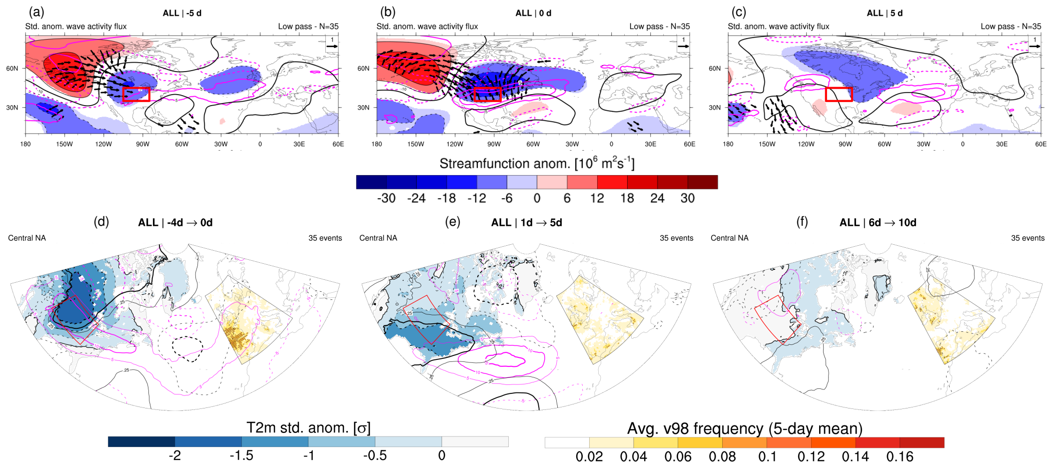

Figure 1. (Top) Lagged composites of 250 hPa wave-activity flux standardized anomalies (arrows), geostrophic streamfunction anomalies (black contours, shaded significant values) and zonal wind anomalies (magenta contours, only $\pm 5\,\mathrm{m\,s^{-1}}$, $\pm 10\,\mathrm{m\,s^{-1}}$, negative values dashed) for the 35 cold spells occurring over the considered central NA region (105°-85°W, 35°-45°N) for (a) t_{CS}-5 d (b) t_{CS}, (c) t_{CS}+5 d. Vectors are shown, and streamfunction anomalies are shaded, only when exceeding the top 99% or bottom 1% of a 2500-times randomly sampled distribution. (Bottom) Composites of extreme (above 98th percentile) 10m wind frequency over Europe, averaged over 5 days, and of standardized 2-meter temperature anomaly over North America and Greenland (notice the two separate color scales) for 5-day periods centered at (d) t_{CS}-2 d, (e) t_{CS}+3 d, (f) t_{CS}+8 d. Overlaid are composites of 250 hPa wind anomaly (magenta contours, only $\pm 5\,\mathrm{m\,s^{-1}}$, $\pm 10\,\mathrm{m\,s^{-1}}$,$\pm 15\,\mathrm{m\,s^{-1}}$), sea level pressure standardized anomaly (black contours, only $\pm 0.25\,\sigma$, $\pm 0.5\,\sigma$), with negative values dashed. Stippling indicates significantly heightened frequency of extreme 5-day-averaged 10m wind with respect to the top 99% or bottom 1% of a 10000-times randomly sampled distribution.

lies over both the British Isles and the Iberian Peninsula (Fig. 1f; see also e.g., Gómara et al., 2014; Messori & Caballero, 2015; Messori et al., 2016). The large-scale configuration projects onto a significantly negative NAO phase in the days preceding the cold spell, but it moves towards more neutral to positive conditions as the cold spell unfolds (Fig. S2a). The anomalous configuration of the upper-level jet stream is also visible using classical jet indices, which indicate a stronger, more equatorward-displaced and zonal jet than usual (as in Figs. Sb-d in the Supplementary Information). The separate trough over western Europe is no longer visible.

In summary, the composites show a wave train upstream of the North American cold spell and the elongation of the North Atlantic jet stream towards western Europe already in the days preceding the cold spell peak, as previously highlighted by Messori et al. (2016). Such a significant anomaly indicates a potential role of North Atlantic storm track dynamics for the genesis of the cold spells; this would however be in apparent contrast, with the role of the North Pacific Rossby wave train as driver of the cold spells, discussed by previous literature.

3.2 Stratification with respect to wave-activity flux

The considerations above suggest a need to compare the relative importance of North Pacific wave trains with respect to the dynamics of the North Atlantic storm track during the cold spells. To verify this, we compute the area-averaged magnitude of the wave-activity flux anomaly vector $|\mathrm{WAF}_{\mathrm{anom}}|$over the considered region (105°-85°W, 35°-45°N) and stratify the same set of cold spells with respect to $|\mathrm{WAF}_{\mathrm{anom}}|$ at cold spell peak. The metric is averaged over the considered cold spell domain, under the assumption that local anomalies in wave-activity flux are indicative of the strength of Rossby wave propagation during the cold spell. We then extract the 12 cold spells associated, respectively, with the top (WAF+) and bottom (WAF-) terciles of $|\mathrm{WAF}_{\mathrm{anom}}|$ and discuss their differences.

A composite analysis shows that cases in the WAF+ subset are indeed characterized by the clear propagation of a Rossby wave train from the North Pacific as the cold spell develops and peaks (Figs. 2a,c). Anomalies in geostrophic streamfunction and wave-activity flux over the north-western portion of North America appear to precede the cold spell also for cases in the WAF- subset, although with a weaker signal than for the WAF+ case (Fig. 2b). The two cold spell subsets are also associated with significantly different flow configurations over the North Atlantic, especially in the days preceding the cold spell (Fig. 2a,b). For WAF+, no significant streamfunction anomalies are visible over the North Atlantic before or during the cold spell peak (Figs. 2a,c). As the wave train propagates over the North Atlantic, the jet tilts poleward over the eastern Atlantic in the direction of the British Isles (Fig. 2e).

The situation is radically different for the WAF- subset. First of all, an anomalous flow pattern resembling a negative NAO phase is visible over the North Atlantic in the days before the cold spell, with an upper-level high over Greenland and two troughs at its southern flanks: one over eastern North America and one over western Europe. Below these, an equatorward-shifted jet is found (Fig. 2b). The unfolding of the WAF- cold spells does not substantially alter the flow configuration over the North Atlantic: the jet remains anomalously equatorward-shifted, and two separate troughs are still visible over the western and eastern parts of the North Atlantic basin (Figs. 2d,f). In this scenario there is no strict need of a precursor North Pacific Rossby wave train: however, the presence of a weak but significant Alaskan ridge in the WAF- composite (Figs. 2b,d) suggests that this feature can still be relevant for particularly intense and/or persistent cold spells.

This analysis explains why central NA cold spells are not followed by a systematically positive or negative NAO (Fig. §3a), as the state of the North Atlantic storm track is conditioned by which dynamical pathway the cold spell is associated with. More pro-

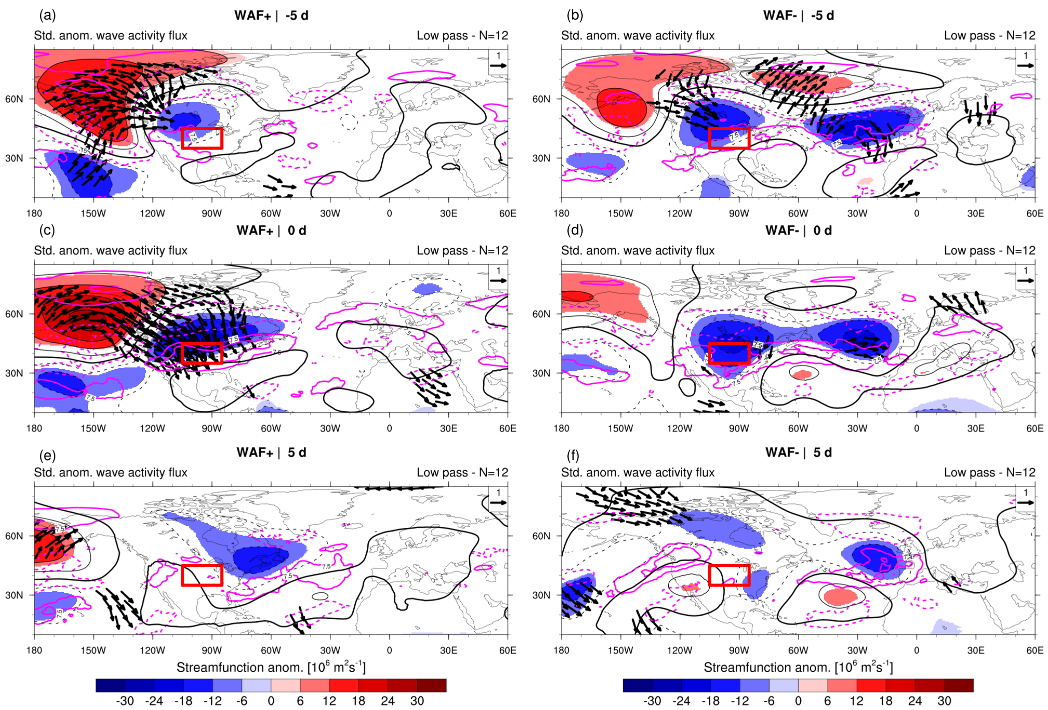

Figure 2. Lagged composites of standardized WAF anomalies (arrows), geostrophic streamfunction anomalies (shaded) and 250 hPa zonal wind anomalies (magenta contours, only $\pm 7.5\,\mathrm{m\,s^{-1}}$, $\pm 15\,\mathrm{m\,s^{-1}}$, negative values dashed) for the 12 central NA cold spells in the (left) WAF+ and (right) WAF- subsets at lags (a,d) t_{CS}-5 d (b,e) t_{CS}, and (c,f) t_{CS}+5 d. Only significant WAF vectors and streamfunction anomalies are shown (with respect to the top 99% or bottom 1% of a 10.000-times randomly sampled distribution).

nounced differences between WAF+ and WAF- emerge when looking at jet speed and latitude, while jet zonality is not systematically different (Figs. §3b-d). As a backward check, we also note that these two distinct dynamical pathways can be re-obtained from a stratification based on the upper and lower terciles of the NAO index four days *after* cold spell peak (see Fig. S4 in the SI). The corresponding 12-cold spell subsets are named NAO+ and NAO-, respectively. The NAO+ cold spells correspond to the NW–SE propagation of a Rossby wave train across North America (Figs. S4a,c), resulting in an enhanced jet stream over the North Atlantic. On the other hand, the NAO- cold spells feature an upper-level anticyclone west of Greenland and an equatorward-shifted jet stream over the Iberian Peninsula already four days before the cold spell peak (Fig. S4b), a situation that remains virtually unchanged as the cold spell unfolds (Figs. S4d,f).

3.3 Implications for surface extremes

The two different dynamical pathways associated with the cold spells are mirrored in differences in the occurrence of European surface wind extremes. In the WAF+ subset, no extreme winds are observed over western Europe preceding the cold spell peak (Figs. 3a,b). This is in sharp contrast with the image gained from the whole subset of the 35 cold spells, which featured a significantly heightened frequency of extreme winds over the Iberian Peninsula and France preceding the cold spell peak (cf. Fig. 1d). On the other hand, the WAF- cold spell subset displays extreme surface winds accompanied by lower than usual sea-level pressure over the Azores and upper-level wind anomalies extending through the whole North Atlantic basin prior to the cold spell peak (Fig. 3d).

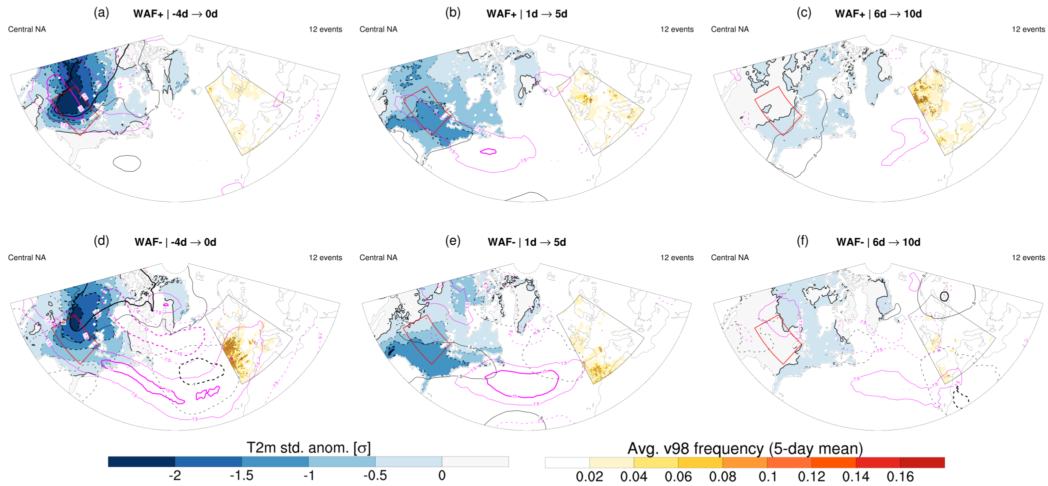

Figure 3. Composites of extreme (above 98th percentile) 10m wind frequency over Europe, averaged over 5 days, and of standardized 2-meter temperature anomaly over North America and Greenland (notice the two separate color scales) following cold spells over central NA belonging to the (top) WAF+ and (bottom) WAF- subsets for the 5-day periods centered at (a,d) t_{CS}-2 d, (b,e) t_{CS}+3 d, (c,f) t_{CS}+8 d. Overlaid are composites of 250 hPa wind anomaly (magenta contours, only $\pm7.5\,\mathrm{m\,s^{-1}}$, $\pm15\,\mathrm{m\,s^{-1}}$), sea level pressure standardized anomaly (black contours, only $\pm0.25\,\sigma$, $\pm0.5\,\sigma$), with negative values dashed. Stippling indicates 5-day-averaged frequencies of extreme 10m wind exceeding the top 99% or bottom 1% of a randomly sampled distribution.

Indeed, extreme surface winds occur mostly in the period preceding, rather than following, the cold spell peak (Figs. 3e,f). The WAF- subset thus appears characterized by *concurrent* developing cold spells over central NA and extreme surface winds over western Europe. This co-occurrence is likely related to the two troughs visible at the entrance and the exit of the North Atlantic storm track (Figs. 2d,f): while the trough to the west advects cold air at its western flank towards the central NA region, the trough to the east is tied to an upper-level jet streak at its southern flank, associated with extreme winds over the Iberian Peninsula (Figs. 3d,e). In addition, the dynamics portrayed in the WAF- subset are consistent with the streamfunction and jet anomalies visible in the full composite (Fig. 1). We thus hypothesize that the puzzling European wind extremes observed *before* the cold spell peak are mostly related to this second pathway for pan-Atlantic cold and windy extremes, in which the North Atlantic storm track is already in a state conducive to European wind extremes before the cold spell peak is reached over Central NA. Given that the Greenland high is likely emerging from the activity of the North Atlantic storm track, it makes sense that its impacts are felt over Europe first (i.e., in term of windstorms), and then upstream over North America (i.e., in terms of large-scale setup leading to cold spells). This mechanism would explain the anticipated wind impact of central NA cold spells noticed by Messori et al. (2016) and Leeding et al. (2022).

4 Concluding remarks

4.1 Summary

Cold spells over central NA are impactful weather events whose occurrence has been empirically related to windstorms over Europe. The underlying hypothesis was that European windstorms were occurring as a "downstream response" of the "upstream" cold spells. The results of this study challenge this view and allow us to conclude that there

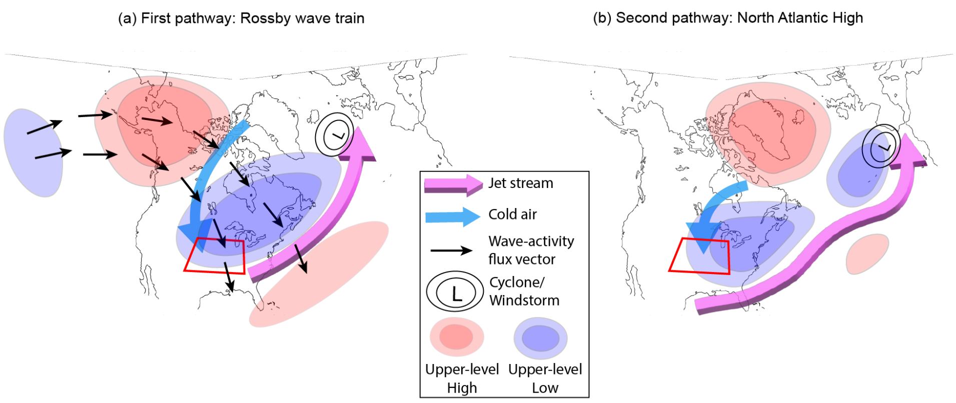

Figure 4. Schematic of the two pathways connecting North American cold spells and European windstorms. (a) In the first pathway, the various upper-level anomalies are related to the propagation of a Rossby wave train from the North Pacific, indicated by the series of thin, black arrows connecting the ridge over Alaska with the trough over eastern North America. (b) In the second pathway, the jet stream is located more equatorward than usual and is associated with anomalous cyclonic activity over south-western Europe.

are at least two possible dynamical pathways to explain the observed statistical link between North American cold spells and European windstorms:

1. Cold spells characterized by the presence of a ridge over Alaska, which is part of a eastward-propagating, low-frequency Rossby wave train, are not associated with significant anomalies over the North Atlantic before cold spell peak. The effect over the North Atlantic storm track manifests itself only when the wave train reaches the eastern portion of the continent, resulting in a tilted, intensified jet stream and in wind extremes over north-western Europe in the 6-10 days following cold spell peak. In this pathway, the propagation of the wave train supports a clear causal link between the circulation pattern causing the cold spell (the Rossby wave train), its impact onto the storm track and the surface wind extremes over Europe (Fig. 4a).
2. The presence of a high west of Greenland is associated with a flow configuration that promotes the development of cold spells over North America and windstorms over Europe at the same time. In particular, the high is often related to the southward displacement of a trough over the eastern United States, which promotes cold air advection at its western flank. At the same time, the large-scale configuration is related to an equatorward shift of the upper-level trough normally associated with the Icelandic Low: this configuration resembles a negative NAO pattern, conducive to extreme winds over south-western Europe (Fig. 4b). As the two weather extremes *co-occur* in time and are associated with a common precursor (the aforementioned Greenland high), it would then be inappropriate to discuss European windstorms as a "downstream effect" of North American cold spells.

In summary, the different drivers of central NA cold spells correspond to different circulation patterns over the North Atlantic, which are then related to an increased frequency of windstorms over different European regions in a physically consistent manner. In the specific case discussed in this study, the original composite picture retained characteristics of the two different drivers at the same time lags, leading to a nonphysical large-scale configuration where the European wind extremes appear to precede the North American cold spell that should cause them. Thus, analyzing pan-Atlantic cold and windy extremes without considering their dynamical drivers can lead to an incomplete, or at worst incorrect, understanding of their dynamics. A similar cautionary argument likely applies to studies concerning temporally and spatially compounding extremes over remote regions (e.g., summer heatwaves or winter cold spells).

4.2 Contextualization of the results and outlook

The two distinct pathways connecting central NA cold spells and European windstorms were identified by stratifying with respect to the area-averaged WAF over the selected cold spell region. Two cold spell subsets were then obtained by selecting the dates corresponding to values in the upper or lower WAF terciles, respectively. Other possible ways to perform this division were attempted, for instance by considering area-averaged wave-activity flux over Alaska, but this choice did not yield a clear division (mainly because not all waves propagating from Alaska engender a cold spell in a given North American region). We thus regard our chosen partition as a simple and physically-grounded way to unravel the different dynamical pathways behind temporally compounding pan-Atlantic cold and windy extremes.

This work focused on a single yet representative North American cold spell domain, but the relative weight of the two pathways likely differs for different regions. Future work will involve a more comprehensive analysis trying to identify differences in the physical connections to European windstorms for cold spells in different North American regions. Another caveat of this analysis is the reduced number of extreme cold spells considered (a total of 35, with 12 cases in the WAF+ and WAF- subsets). We nonetheless underscore the high level of statistical significance of our results. Furthermore, we did not analyse possible remote drivers behind the two identified pathways. Possible candidates are tropical convection anomalies over SE Asia and the maritime continent, which have been linked to the forcing of Rossby wave trains over the Pacific Ocean (e.g., Teng & Branstator, 2017; Riboldi et al., 2022), or the occurrence of sudden stratospheric warmings, which have been connected with the formation of high-latitude anticyclones and with an equatorward displacement of the jet stream over the North Atlantic basin (e.g., Kolstad et al., 2022).

The chosen central NA region is located roughly in the middle between the Pacific and the Atlantic Oceans, and the two identified pathways for pan-Atlantic cold and windy extremes reflect the role played by the basins. The first pathway features a strong wave propagation from the upstream North Pacific, while the second one appears more influenced by high-latitude upper-level ridges over Greenland and the Canadian Arctic, that plausibly result from the dynamics of the North Atlantic storm track (e.g., atmospheric blocking following explosive cyclogenesis). This indicates that both basins can play a role in the genesis of central NA cold spells, as hinted by Lee et al. (2019) and recently emphasized by Millin et al. (2022) using a weather regime approach. This conceptualization has now been extended to the North Atlantic basin, so that pan-Atlantic wet and windy extremes can be seamlessly understood as part of individual large-scale flow configurations tied to the activity of the Pacific and Atlantic storm tracks. In conclusion, this study provided an interesting case-study of the role played by hemispheric-scale teleconnections in coordinating extreme weather events across North America and Europe, paving the way to frameworks for the prediction and mitigation of their joint impacts.

5 Open Research

ERA5 hourly data from 1979-present are available for several pressure levels (Hersbach et al., 2018a) and for surface variables (Hersbach et al., 2018b). Both data sets were freely downloaded from the Copernicus Climate Change Service (C3S) Climate Data Store.

Acknowledgments

JR, RL and GM acknowledge funding from the European Research Council (ERC) under the European Union's Horizon 2020 research and innovation program (grant agreement no. 948309, CENÆ project). The authors also wish to thank Paolo Ghinassi for the helpful discussions about properties of the wave-activity flux.

References

Benedict, J. J., Lee, S., & Feldstein, S. B. (2004). Synoptic view of the North Atlantic Oscillation. *J. Atmos. Sci.*, *61*, 121–144. doi: 10.1175/1520-0469(2004)061⟨0121:SVOTNA⟩2.0.CO;2

Brayshaw, D. J., Hoskins, B., & Blackburn, M. (2009). The basic ingredients of the North Atlantic storm track. Part I: Land–sea contrast and orography. *J. Atmos. Sci.*, *66*, 2539–2558. doi: 10.1175/2009JAS3078.1

Carrera, M. L., Higgins, R. W., & Kousky, V. E. (2004). Downstream weather impacts associated with atmospheric blocking over the northeast pacific. *J. Climate*, *17*, 4823–4839. doi: 10.1175/JCLI-3237.1

Cellitti, M. P., Walsh, J. E., Rauber, R. M., & Portis, D. H. (2006). Extreme cold air outbreaks over the United States, the polar vortex, and the large-scale circulation. *J. Geophys. Res.: Atmospheres*, *111*, D02114. doi: https://doi.org/10.1029/2005JD006273

Dickson, R. R., & Namias, J. (1976). North American influences on the circulation and climate of the North Atlantic sector. *Mon. Wea. Rev.*, *104*, 1255–1265. doi: 10.1175/1520-0493(1976)104⟨1255:NAIOTC⟩2.0.CO;2

Franzke, C., Lee, S., & Feldstein, S. B. (2004). Is the North Atlantic Oscillation a breaking wave? *J. Atmos. Sci.*, *61*, 145–160. doi: 10.1175/1520-0469(2004)061⟨0145:ITNAOA⟩2.0.CO;2

Gómara, I., Rodríguez-Fonseca, B., Zurita-Gotor, P., & Pinto, J. G. (2014). On the relation between explosive cyclones affecting europe and the North Atlantic Oscillation. *Geophys. Res. Lett.*, *41*, 2182–2190. doi: https://doi.org/10.1002/2014GL059647

Held, I. M. (1983). Stationary and quasi-stationary eddies in the extratropical troposphere: Theory. In B. J. Hoskins & R. P. Pearce (Eds.), *Large-Scale Dynamical Processes in the Atmosphere* (pp. 127–168). Academic Press.

Hersbach, H., Bell, B., Berrisford, P., Biavati, G., Horányi, A., Muñoz Sabater, J., . . . Thépaut, J.-N. (2018a). *ERA5 hourly data on pressure levels from 1959 to present.* [dataset]. Copernicus Climate Change Service (C3S) Climate Data Store (CDS). Retrieved from `https://cds.climate.copernicus.eu/cdsapp#!/dataset/reanalysis-era5-pressure-levels?tab=form` doi: 10.24381/cds.bd0915c6

Hersbach, H., Bell, B., Berrisford, P., Biavati, G., Horányi, A., Muñoz Sabater, J., . . . Thépaut, J.-N. (2018b). *ERA5 hourly data on single levels from 1959 to present.* [dataset]. Copernicus Climate Change Service (C3S) Climate Data Store (CDS). Retrieved from `https://cds.climate.copernicus.eu/cdsapp#!/dataset/reanalysis-era5-single-levels?tab=form` doi: 10.24381/cds.adbb2d47

Hersbach, H., Bell, B., Berrisford, P., Hirahara, S., Horányi, A., Muñoz-Sabater, J., . . . Thépaut, J.-N. (2020). The ERA5 global reanalysis. *Quart. J. Roy. Meteor. Soc.*, *146*, 1999–2049. doi: https://doi.org/10.1002/qj.3803

Huntingford, C., Marsh, T., Scaife, A. A., Kendon, E. J., Hannaford, J., Kay, A. L., . . . Allen, M. R. (2014). Potential influences on the United Kingdom's floods of winter 2013/14. *Nature Clim Change*, *4*, 769–777. doi: 10.1038/nclimate231

Karremann, M. K., Pinto, J. G., Reyers, M., & Klawa, M. (2014). Return periods of losses associated with european windstorm series in a changing climate. *En-*

viron. Res. Lett., *9*, 124016. doi: 10.1088/1748-9326/9/12/124016

Klawa, M., & Ulbrich, U. (2003). A model for the estimation of storm losses and the identification of severe winter storms in Germany. *Nat. Hazards Earth Syst. Sci.*, *3*, 725–732. doi: 10.5194/nhess-3-725-2003

Knight, J. R., Maidens, A., Watson, P. A. G., Andrews, M., Belcher, S., Brunet, G., ... Slingo, J. (2017). Global meteorological influences on the record UK rainfall of winter 2013–14. *Env. Res. Lett.*, *12*, 074001. doi: 10.1088/1748-9326/aa693c

Kolstad, E. W., Lee, S. H., Butler, A. H., Domeisen, D. I. V., & Wulff, C. O. (2022). Diverse surface signatures of stratospheric polar vortex anomalies. *J. Geophys. Res.: Atmospheres*, *127*, e2022JD037422. doi: https://doi.org/10.1029/2022JD037422

Lee, S. H., Furtado, J. C., & Charlton-Perez, A. J. (2019). Wintertime North American weather regimes and the Arctic stratospheric polar vortex. *Geophys. Res. Lett.*, *46*, 14892–14900. doi: https://doi.org/10.1029/2019GL085592

Leeding, R., Riboldi, J., & Messori, G. (2022). On pan-Atlantic cold, wet and windy compound extremes. *Wea. Clim. Extremes*. (in press) doi: doi.org/10.1016/j.wace.2022.100524

Messori, G., & Caballero, R. (2015). On double Rossby wave breaking in the North Atlantic. *J. Geophys. Res.: Atmospheres*, *120*, 11,129–11,150. doi: 10.1002/2015JD023854

Messori, G., Caballero, R., & Gaetani, M. (2016). On cold spells in North America and storminess in western Europe. *Geophys. Res. Lett.*, *43*(12), 6620–6628. doi: 10.1002/2016GL069392

Millin, O. T., Furtado, J. C., & Basara, J. B. (2022). Characteristics, evolution, and formation of cold air outbreaks in the great plains of the united states. *J. Climate*, *35*, 4585–4602. doi: 10.1175/JCLI-D-21-0772.1

Mills, E. (2005). Insurance in a climate of change. *Science*, *309*, 1040–1044. doi: 10.1126/science.1112121

Owen, L. E., Catto, J. L., Stephenson, D. B., & Dunstone, N. J. (2021). Compound precipitation and wind extremes over europe and their relationship to extratropical cyclones. *Wea. Clim. Extremes*, *33*, 100342. doi: https://doi.org/10.1016/j.wace.2021.100342

Palmer, T. (2014). Record-breaking winters and global climate change. *Science*, *344*, 803–804. doi: 10.1126/science.1255147

Portal, A., Pasquero, C., D'Andrea, F., Davini, P., Hamouda, M. E., & Rivière, G. (2022). Influence of reduced winter land-sea contrast on the mid-latitude atmospheric circulation. *J. Climate*. (in press) doi: 10.1175/JCLI-D-21-0941.1

Riboldi, J., Rousi, E., D'Andrea, F., Rivière, G., & Lott, F. (2022). Circumglobal rossby wave patterns during boreal winter highlighted by space–time spectral analysis. *Weather Clim. Dynam.*, *3*, 449–469. doi: 10.5194/wcd-3-449-2022

Rivière, G., & Drouard, M. (2015). Dynamics of the Northern Annular Mode at weekly time scales. *J. Atmos. Sci.*, *72*, 4569–4590. doi: 10.1175/JAS-D-15-0069.1

Rivière, G., & Orlanski, I. (2007). Characteristics of the Atlantic storm-track eddy activity and its relation with the North Atlantic Oscillation. *J. Atmos. Sci.*, *64*, 241–266. doi: 10.1175/JAS3850.1

Ryti, N. R., Guo, Y., & Jaakkola, J. J. (2016). Global association of cold spells and adverse health effects: A systematic review and meta-analysis. *Environ. Health Perspect.*, *124*, 12–22. doi: 10.1289/ehp.1408104

Schemm, S., Rivière, G., Ciasto, L. M., & Li, C. (2018). Extratropical cyclogenesis changes in connection with tropospheric ENSO teleconnections to the North Atlantic: Role of stationary and transient waves. *J. Atmos. Sci.*, *75*, 3943–3964. doi: 10.1175/JAS-D-17-0340.1

Smith, E. T., & Sheridan, S. C. (2019). The influence of atmospheric circulation patterns on cold air outbreaks in the eastern United States. *Int. J. Climatol.*, *39*, 2080–2095. doi: https://doi.org/10.1002/joc.5935

Takaya, K., & Nakamura, H. (1997). A formulation of a wave-activity flux for stationary Rossby waves on a zonally varying basic flow. *Geophys. Res. Lett.*, *24*, 2985–2988. doi: https://doi.org/10.1029/97GL03094

Teng, H., & Branstator, G. (2017). Causes of extreme ridges that induce California droughts. *J. Climate*, *30*, 1477–1492. doi: 10.1175/JCLI-D-16-0524.1

Wolf, G., & Wirth, V. (2017). Diagnosing the horizontal propagation of Rossby wave packets along the midlatitude waveguide. *Mon. Wea. Rev.*, *145*, 3247–3264. doi: 10.1175/MWR-D-16-0355.1

Xie, Z., Black, R. X., & Deng, Y. (2017). The structure and large-scale organization of extreme cold waves over the conterminous United States. *Clim. Dyn.*, *49*, 4075–4088. doi: 10.1007/s00382-017-3564-6

Zscheischler, J., Martius, O., Westra, S., Bevacqua, E., Raymond, C., Horton, R. M., . . . Vignotto, E. (2020). A typology of compound weather and climate events. *Nat. Rev. Earth Environ.*, *1*, 333–347. doi: 10.1038/s43017-020-0060-z

Supporting Information for "Multiple large-scale dynamical pathways for pan–Atlantic compound cold and windy extremes"

Jacopo Riboldi[1], Richard Leeding[1], Antonio Segalini[1], Gabriele Messori[1,2,3]

[1]Department of Earth Sciences, Uppsala University, Uppsala, Sweden

[2]Centre of natural Hazards and Disaster Science (CNDS), Uppsala University, Uppsala, Sweden

[3]Department of Meteorology and Bolin Centre for Climate Research, Stockholm University, Stockholm, Sweden

Contents of this file

1. Text S1
2. Figures S1 to S4
3. Tables S1

Introduction

This Supporting Information contains:

- a detailed description of the computation and the filtering of wave activity flux;
- four supplementary figures that integrate the results exposed in the paper;
- a table with the list of analyzed North American cold spells.

Text S1. Notes about wave-activity flux computation and filtering The computation of the wave-activity flux is based on ERA5 geopotential and wind data, using a NCAR Command Language (NCL) script developed by Kazuaki Nishii, publicly available at http://www.atmos.rcast.u-tokyo.ac.jp/nishii/programs/index.html. It is based on anomalies of geostrophic streamfunction at 250 hPa

$$\psi' = \Phi'_{250}/f \tag{1}$$

where Φ'_{250} is the geopotential ($\Phi = gz$) anomaly at the same level and f is the latitude-dependent Coriolis parameter. Anomalies are obtained with respect to the seasonal cycle, calculated from the 30-day-running mean of geopotential for each calendar day. The two horizontal components of the wave activity flux $\mathbf{WAF} = (\mathrm{WAF}_x, \mathrm{WAF}_y)$ are then defined as

$$\mathrm{WAF}_x = \frac{p}{1000}\frac{1}{2|\mathbf{U}|a^2}\left\{\frac{U}{\cos\phi}\left[\left(\frac{\partial\psi'}{\partial\lambda}\right)^2 - \psi'\frac{\partial^2\psi'}{\partial\lambda^2}\right] + V\left[\frac{\partial\psi'}{\partial\lambda}\frac{\partial\psi'}{\partial\phi} - \psi'\frac{\partial^2\psi'}{\partial\psi\partial\phi}\right]\right\} \tag{2}$$

$$\mathrm{WAF}_y = \frac{p}{1000}\frac{1}{2|\mathbf{U}|a^2}\left\{\left[U\frac{\partial\psi'}{\partial\lambda}\frac{\partial\psi'}{\partial\phi} - \psi'\frac{\partial^2\psi'}{\partial\psi'\partial\phi}\right] + V\cos\phi\left[\left(\frac{\partial\psi'}{\partial\phi}\right)^2 - \psi'\frac{\partial^2\psi'}{\partial\phi^2}\right]\right\} \tag{3}$$

where λ is the longitude, ϕ is the latitude and $|\mathbf{U}| = (U, V)$ is the background climatology of the zonal and meridional component of the wind at 250 hPa, also obtained from the 30-day-smoothed seasonal cycle. As we are considering only the slow-moving, low-frequency flow component, we neglect here the additional term corresponding to the phase propagation of the wave in the direction of the background wind (present instead in the formulation of Takaya & Nakamura, 2001).

Given that the **WAF** field resulting from the computation featured variations at a very small scale (which is inconsistent with the applied low-pass time filtering, as noticed by

Wolf & Wirth, 2017), a truncation based on spherical harmonics was further applied to eliminate numerical noise. This filter exploited the spatial coherence of planetary-scale motions providing a sufficiently smooth spatial field at every instant. The **WAF** field at a given pressure level was first projected in a space spanned by spherical harmonics, $Y_n^m(\phi, \lambda)$, by means of the Python routine shtns (Schaeffer, 2013). The filtering is then performed by suppressing all the components with degree $n > 20$, corresponding to eliminating all variations with wavenumber larger than 20 in both the zonal and meridional direction. The filtered spatial field was constructed by inverting the modified spherical harmonics projection. Figure S1 shows an example of the resulting filtered field from a WAF_x spatial field where it can be clearly observed that the filter keeps the large coherent features and removes the fine-grained noise, facilitating the assessment of the wave activity flux.

References

Schaeffer, N. (2013). Efficient spherical harmonic transforms aimed at pseudospectral numerical simulations. *Geochemistry, Geophysics, Geosystems*, *14*(3), 751–758.

Takaya, K., & Nakamura, H. (2001). A formulation of a phase-independent wave-activity flux for stationary and migratory quasigeostrophic eddies on a zonally varying basic flow. *J. Atmos. Sci.*, *58*, 608 - 627. doi: 10.1175/1520-0469(2001)058⟨0608:AFOAPI⟩2.0.CO;2

Wolf, G., & Wirth, V. (2017). Diagnosing the horizontal propagation of Rossby wave packets along the midlatitude waveguide. *Mon. Wea. Rev.*, *145*, 3247–3264. doi: 10.1175/MWR-D-16-0355.1

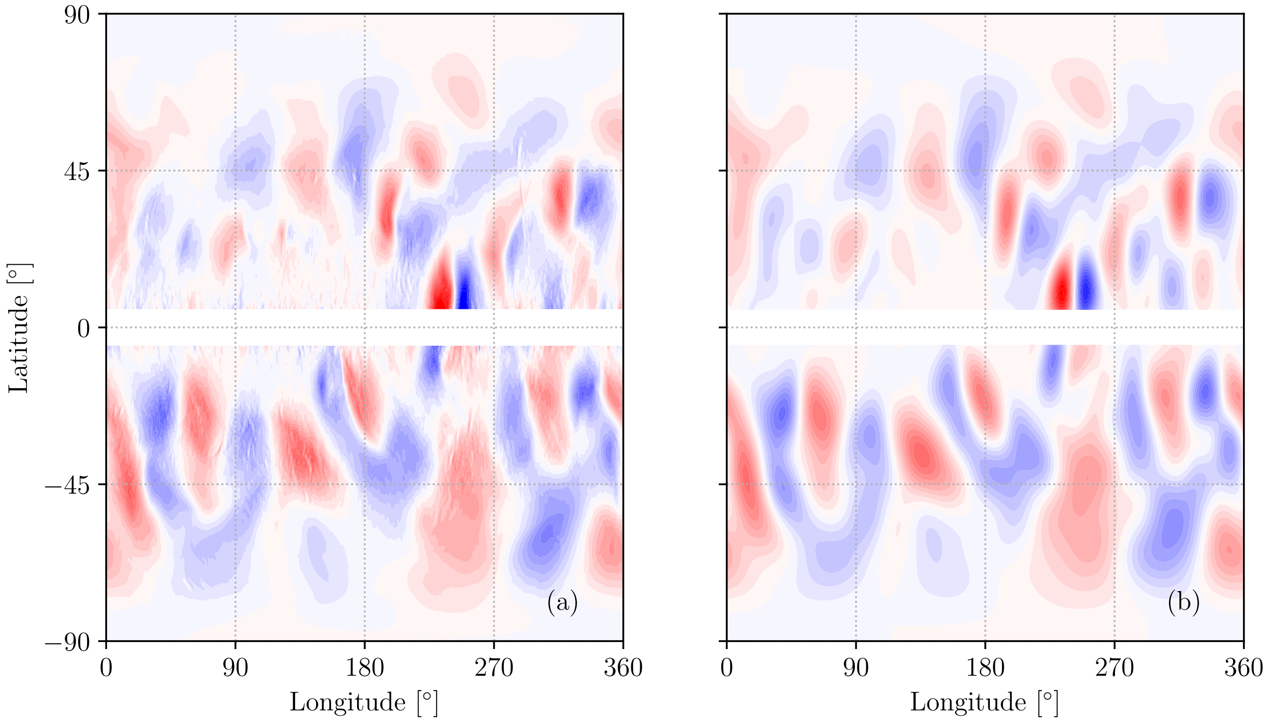

Figure S1. Comparison between (a) the WAF_x field for the 24. Dec. 1979 and (b) its filtered version.

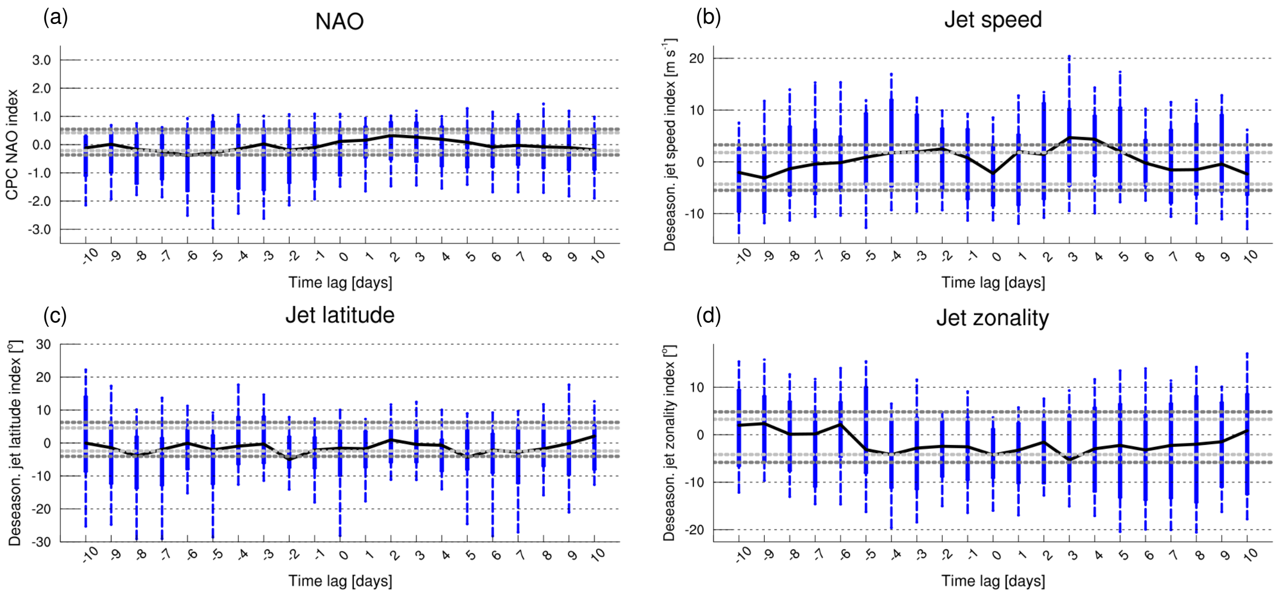

Figure S2. Distributions of (a) North Atlantic Oscillation (NAO), (b) jet speed (c) jet latitude and (d) jet zonality indices for the considered 35 Central NA cold spells (in blue). The lower (upper) whisker marks the lower (upper) decile of each distribution. The black bold line connects the medians at each time step, while the lower (upper) bound of the box indicates the lower (upper) quartile. The dark (light) grey dotted lines refer to the top/bottom 1% (5%) of a 10.000-times randomly resampled distribution of the same quantity.

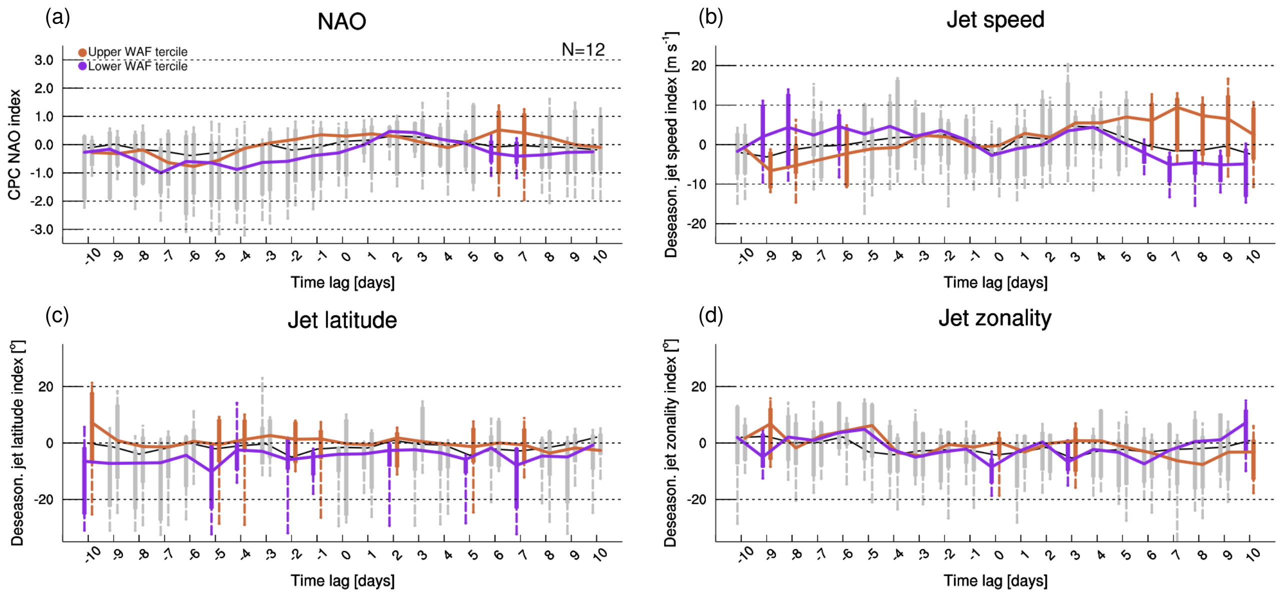

Figure S3. Distributions of (a) North Atlantic Oscillation (NAO), (b) jet speed (c) jet latitude and (d) jet zonality indices for the 12 Central NA cold spells in the WAF+ (orange) and WAF- (indigo) subsets. Only time lags with a difference between the subset medians in the top/bottom 5% of a 10.000-times random reshuffling of the two subsets are colored. Box-and-whiskers diagrams as in Fig. S2.

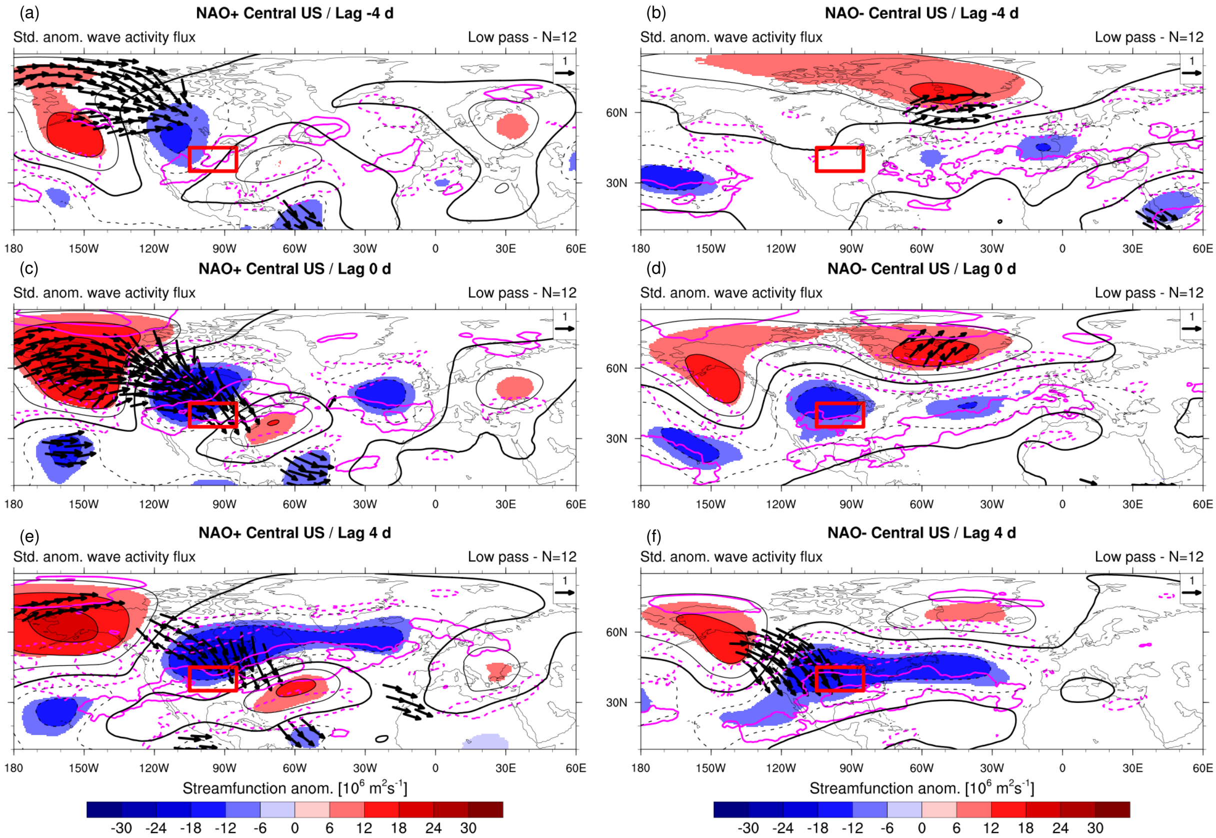

Figure S4. Lagged composited of standardized WAF anomalies (arrows), geostrophic stream-function anomalies (shaded) and 250 hPa zonal wind anomalies (magenta contours, only $\pm 5\,\mathrm{m\,s^{-1}}$, $\pm 10\,\mathrm{m\,s^{-1}}$, negative values dashed) for the 12 central NA cold spells in the (left) NAO+ and (right) NAO- subsets at lags (a,d) t_{CS}-4 d (b,e) t_{CS}, and (c,f) t_{CS}+4 d. Only significant WAF vectors and streamfunction anomalies are shown (with respect to the top 99% or bottom 1% of a bootstrapped distribution).

Table S1. List of 35 cold spells in the Central North America region considered in this study, ordered with respect to the area-averaged wave activity flux (WAF) in the region. Cold spells belonging to the upper (WAF+) and lower (WAF-) tercile subsets are indicated in the last column.

Number	Date	WAF [$10^6\,m^2\,s^{-2}$]	Subset
1	1985-02-02	142.67	WAF+
2	2013-12-08	82.61	WAF+
3	1990-12-24	61.80	WAF+
4	1989-02-05	53.30	WAF+
5	1994-01-17	33.96	WAF+
6	2006-02-19	33.68	WAF+
7	2010-01-07	32.24	WAF+
8	1982-02-08	29.39	WAF+
9	1983-12-24	26.16	WAF+
10	2018-01-01	24.57	WAF+
11	1993-02-18	22.57	WAF+
12	1980-01-29	22.31	WAF+
13	2008-01-22	22.28	
14	2006-12-02	19.31	
15	2003-01-24	19.28	
16	2005-12-07	19.01	
17	1984-01-19	18.85	
18	2009-01-26	18.30	
19	1983-12-01	17.75	
20	2015-02-21	17.37	
21	2009-12-09	16.51	
22	1991-12-03	15.93	
23	2011-02-09	15.89	
24	1982-01-11	15.83	WAF-
25	1981-02-11	12.97	WAF-
26	2014-02-08	12.45	WAF-
27	2000-12-13	12.35	WAF-
28	1989-12-21	12.11	WAF-
29	1997-01-12	10.64	WAF-
30	2003-02-25	9.87	WAF-
31	1985-12-01	8.46	WAF-
32	1986-02-11	7.45	WAF-
33	2007-02-15	7.03	WAF-
34	1988-01-07	5.99	WAF-
35	1996-02-02	5.28	WAF-